Table 1. Summarized features of recombinant ALAS2 proteins

Recombinant protein	In vitro enzymatic activity (nmol ALA/mg protein/h)			Half-life in HEK293 cells (h)	Porphyrin accumulation in HEK293 cells
	Without PLP (% of wild-type)	With 200 μM PLP (% of wild-type)	Ratio with/without PLP		
Wild-type	14,824 ± 754 (100%)	27,627 ± 713 (100%)	1.86	7.8	+++
Val562Ala	22,324 ± 1,555 (150.6%)	32,300 ± 709 (116.9%)	1.44	5.3	++
Met567Ile	5,653 ± 897 (38.1%)	6,975 ± 299 (25.2%)	1.23	>12	±
Ser568Gly*	(19.5%)*	(31.6%)*	2.51*	>12	±
delC33	15,769 ± 382 (106.4%)	53,066 ± 1,843 (192.1%)	3.37	>12	++++

*Data with GST-fused Ser568Gly protein taken from reference [15].

Results

Identification of novel mutations of ALAS2 gene

Analyzing the genomic DNA extracted from the proband of case 1, we identified the c.T1685C mutation in the 11th exon of ALAS2 gene (Supplementary Figure E1A, upper panel; online only, available at www.exphem.org). This transition results in an amino acid substitution at the 562nd residue of ALAS2 protein from valine to alanine (Val562Ala). The same mutation was identified in one allele of the proband's mother (Supplementary Figure E1A, middle panel; online only, available at www.exphem.org), and the proband's father does not carry this mutation (Supplementary Figure E1A, lower panel; online only, available at www.exphem.org), indicating the X-linked inheritance of this mutation. For the proband of case 2, the c.G1701C transversion was identified in exon 11 of ALAS2 gene (Supplementary Figure E1B; online only, available at www.exphem.org), the mutation of which results in an amino acid substitution at the 567th residue from methionine to isoleucine (Met567Ile).

To exclude the possibility that these mutations represent single nucleotide polymorphisms, we examined the 11th exon of ALAS2 gene in 96 Japanese healthy volunteers (57 male and 39 female subjects, with the total allele number of 135) using PCR followed by direct sequencing. As a result, no base change was found in the 11th exon of ALAS2 gene in these subjects, suggesting that the mutation found in each proband might not represent single nucleotide polymorphism. It is therefore conceivable that either the c.T1685C or c.G1701C mutation might be responsible for XLSA.

Enzymatic activities of mutant ALAS2 proteins in vitro

Wild-type ALAS2 or each mutant ALAS2 protein was expressed in *E. coli* and purified as a tag-free protein. The combination of pTXB1 expression vector and IMPACT system allowed us to obtain a tag-free/C-terminal intact recombinant protein. Indeed, modified Coomassie Brilliant Blue staining of the gel after SDS-PAGE revealed that the purity of each prepared protein was >95% (data not shown). These recombinant proteins were suitable for determination of the catalytic activity of each mutant protein that carries the amino acid substitution near the C-terminal end.

We measured the catalytic activity of each recombinant ALAS2 protein with or without pyridoxal 5-phosphate (PLP). Data are summarized in Table 1. Unexpectedly, the catalytic activity of Val562Ala protein was significantly higher than that of wild-type protein ($p = 0.0046$), when the activity was measured without PLP in the assay mixture. In addition, in the presence of 200 μM PLP, Val562Ala mutant showed significantly higher activity than that of wild-type ALAS2 ($p = 0.0087$). In contrast, the catalytic activity of Met567Ile protein was lower than that of wild-type protein, irrespective of without PLP ($p = 0.0011$) or with PLP ($p = 0.0003$). It is also noteworthy that the PLP-associated increases in enzymatic activities were 86%, 44%, and 23% for wild-type, Val562Ala, and Met567Ile proteins, respectively, suggesting that Val562Ala and Met567Ile mutations decreased the responsiveness to PLP (Table 1). The lowest PLP responsiveness of Met567Ile mutant protein might account for the clinical course of the proband in case 2; that is, the anemia of this proband was improved only marginally, despite pyridoxine treatment.

Because we previously reported on the Ser568Gly mutation [15], which is also located in the C-terminal region of human ALAS2 protein, the reported data for the Ser568Gly mutation were included as a reference in Table 1. In vitro enzymatic activity of glutathione *S*-transferase (GST)–fused Ser568Gly was significantly lower than that of the GST–fused wild-type ALAS2 with or without PLP [15]. Therefore, the functional consequence of amino acid substitution at Ser568 was similar to that of Met567Ile (Table 1). In addition, the degree of PLP-mediated increase in Ser568Gly activity, indicated as "ratio with/without PLP" in Table 1, was larger than that with wild-type protein, although the possibility remains that the GST tag might have influenced the PLP responsiveness of a recombinant ALAS2 protein. We, therefore, included Ser568Gly mutant in subsequent analyses.

The higher catalytic activity of Val562Ala protein prompted us to examine the function of the C-terminal region of ALAS2 protein. We measured the enzymatic

activity of the deletion mutant that lacks the 33 amino acids at the C-terminal end (positions 555–587) of human ALAS2 (delC33 mutant), the region of which was conserved among mammalian ALAS2 proteins, including Val562. As shown in Table 1, the enzymatic activity of the delC33 mutant was higher by two times in the presence of PLP than that of wild-type ALAS2 ($p = 0.002$), whereas they showed similar enzymatic activity in the absence of PLP. These results suggest that the 33 amino acids at the C-terminal end of human ALAS2 protein might repress the enzymatic activity, probably by interfering with the access of PLP cofactor to the catalytic site.

Stability of mutant ALAS2 proteins in vivo

We were interested in studying how the Val562Ala mutation is associated with XLSA, despite higher enzymatic activity. We examined the stability of the Val562Ala mutant protein and other C-terminal mutant proteins in vivo. When human ALAS2 protein is expressed as a FLAG-tagged protein in eukaryotic cells, the precursor and mature proteins should be detected as 65.7-kDa and 60.5-kDa proteins, respectively. As shown in Figure 1B (upper panel) and Figure 2 (middle panel), FLAG-tagged wild-type ALAS2 and mutant ALAS2 proteins, except for delC33 mutant, were detected as bands at about 60 kDa, an expected size of the mature protein. These results suggest that the leader peptide at the N-terminal end was cleaved after translocation of the precursor protein into mitochondria [4]. In fact, the precursor protein was detected at an expected size, when HeLa cells were transfected with FLAG-ALAS2 expression vector, and then incubated with hemin (Supplementary Figure E2; online only, available at www.exphem.org), which is known to inhibit mitochondrial translocation of ALAS precursor protein into mitochondria [4]. Based on our experiments (Fig. 1A–C), the half-lives of wild-type and Val562Ala mature proteins in mitochondria were calculated as 7.8 hours and 5.3 hours, respectively. The half-life of the Val562Ala mutant protein (Fig. 1C) is shorter than that of wild-type ALAS2 protein (Fig. 1B). In contrast, the half-life of Met567Ile (Fig. 1D) or Ser568Gly (Fig. 1E) mutant was not measurable by our experiments because the 50% reduction of the protein level was not observed within 12 hours for these mutants. Thus, the half-lives of Met567Ile and Ser568Gly mutants were longer than 12 hours. Importantly, the amino acid substitutions in the C-terminal region influenced the stability of the mature ALAS2 protein in mitochondria in different manners. Namely, Val562Ala mutation results in destabilization of the mature protein, and either Met567Ile or Ser568Gly mutation stabilizes the mature protein in mitochondria.

In addition, we measured the half-life of delC33 mutant in HEK293-derived cells (Fig. 1F), showing that the 50% reduction was not observed within 12 hours, which was similar to Met567Ile and Ser568Gly mutants. These results suggested that the 33 amino acids at C-terminal region of ALAS2 protein suppressed the catalytic activity in vitro, as well as protein stability in mitochondria. Our data also indicate that Val562Ala mutation might enhance the destabilization function of the C-terminal region, whereas Met567Ile and Ser568Gly mutations might enhance the suppressive function for enzymatic activity.

Enzymatic activity of each ALAS2 mutant protein in vivo

Val562Ala mutant showed higher enzymatic activity in vitro (Table 1), but it was less stable in mitochondria (Fig. 1A) compared with wild-type ALAS2. On the other hand, Met567Ile and Ser568Gly mutants showed lower enzymatic activities in vitro (Table 1), with prolonged half-lives in mitochondria (Fig. 1A). We, therefore, determined the catalytic activity of each mutant protein in vivo. For this purpose, we compared the accumulation of porphyrins in HEK293-derived cells that expressed wild-type protein or a mutant protein, as we described previously [20]; that is, the accumulation of porphyrins was evaluated by comparing the intensity of the fluorescence under ultraviolet light (Fig. 2, upper panel). The accumulation of porphyrins was detected in cells expressing wild-type ALAS2, but not in cells expressing tagged luciferase. These results indicate that FLAG-tagged ALAS2 is catalytically active in mitochondria. In contrast, the accumulation of porphyrins was decreased in cells expressing Val562Ala, Met567Ile, or Ser568Gly protein, compared to cells expressing wild-type ALAS2. Among these three missense mutations, Val562Ala mutant showed higher catalytic activity than did Met567Ile or Ser568Gly mutant (Fig. 2, upper panel). In addition, the highest porphyrin accumulation was observed in cells expressing delC33. Of note, the expression level of Val562Ala mutant protein was much lower than that of any other mutant or wild-type ALAS2, as judged by Western blot analysis (Fig. 2, middle panel), although there was no significant difference in relative expression level of each mutant ALAS2 messenger RNA (Fig. 2, lower panel). These results suggest that Val562Ala mutant protein is catalytically hyperactive but unstable in mitochondria, which is consistent in part with the higher enzymatic activity detected in vitro (Table 1) and with the short-half life in vivo (Fig. 1A).

In conclusion, Val562Ala, Met567Ile, or Ser568Gly ALAS2 has lower enzymatic activity in mitochondria compared with the activity of wild-type ALAS2. Therefore, these three mutations are categorized as a loss-of-function mutation and are responsible for sideroblastic anemia.

Discussion

It is well known that a loss-of-function mutation of the ALAS2 gene causes XLSA. In addition to the ALAS2 gene, other genes (e.g., SLC25A38 [24], GLRX5 [25], ABCB7 [26], PUS1 [27], SLC19A2 [28], and mitochondrial DNA [29]) were reported to be responsible for

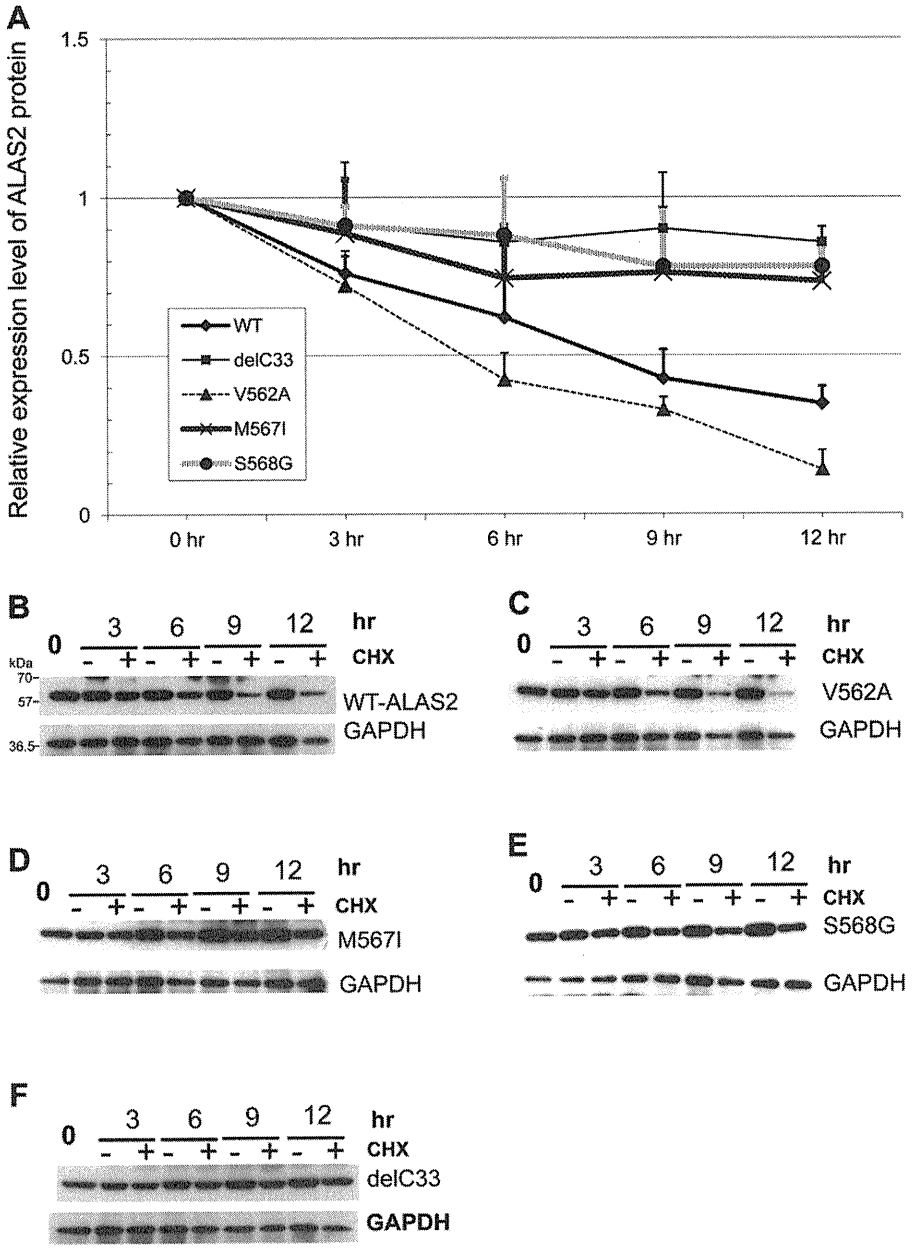

Figure 1. Effect of cycloheximide on FLAG-tagged ALAS2 protein level in eukaryotic cells. Expression of each FLAG-tagged protein was induced with tetracycline (1 μg/mL) in HEK293-derived cells for 48 hours, and then cells were treated with 10 μg/mL cycloheximide (CHX) for the indicated hours. Cells were collected and lysed in RIPA buffer, and FLAG-tagged proteins were detected by Western blot analysis (**B**–**F**). The intensity of the FLAG-tagged protein was normalized with the intensity of GAPDH for each time point. In (**A**), the relative intensity representing FLAG-tagged protein at 0 hours was considered to be 100%. The half-life of each protein was calculated on the basis of 50% reduction of each protein expression from the relative expression curves obtained from the samples with CHX. Average value of three independent experiments was used for preparing (**A**). Representative data of each ALAS2 protein are shown (**B**–**F**): (**B**) wild-type (WT) ALAS2; (**C**) Val562Ala; (**D**) Met567Ile; (**E**) Ser568Gly; and (**F**) delC33.

hereditary or congenital sideroblastic anemia. Among these candidate genes, mutations in ALAS2 gene are most frequently identified in patients with sideroblastic anemia [30], but characterization of each mutant ALAS2 protein was not fully performed. To the best of our knowledge, 24 of 56 mutations of the ALAS2 gene were characterized in vitro using recombinant proteins with or without a peptide-tag [9,10,14,15,20,21,31–36]. In the 11th exon of the ALAS2 gene, Ser568Gly [15], Arg559His [17], Arg560His [16], and Arg572His [14] mutations have been reported; however, only Ser568Gly and Arg572His mutants were characterized using recombinant proteins. Concerning the Ser568Gly mutation [15], we confirmed that Ser568Gly mutation resulted in decreased enzymatic activity in vitro (about 30% of wild-type with PLP in the assay mixture), as shown in Table 1. In contrast, Ducamp et al. [14] were

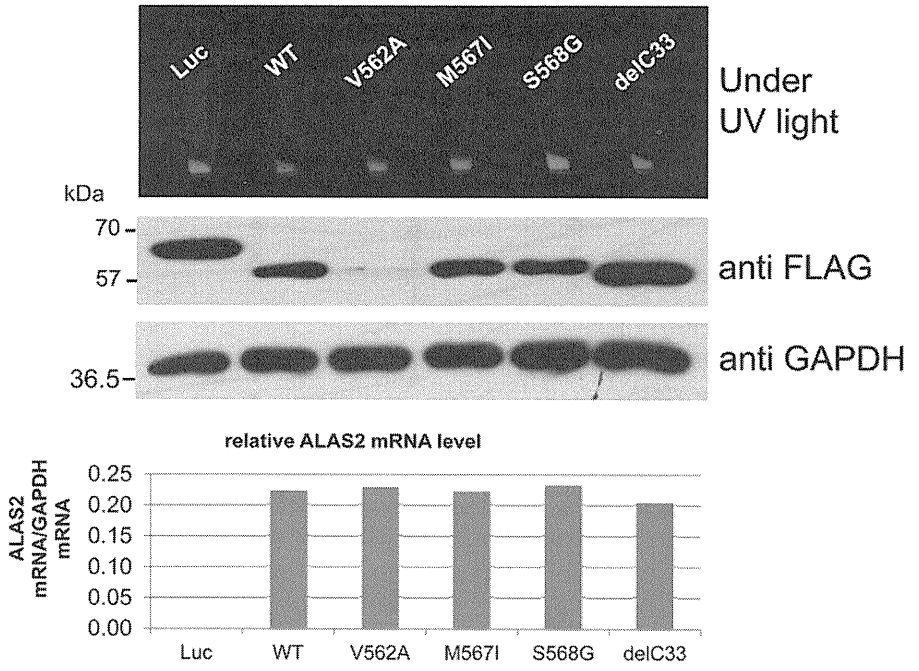

Figure 2. Evaluation of porphyrin production in cells expressing each ALAS2 mutant protein. Each FLAG-tagged ALAS2 protein or FLAG-tagged luciferase protein as a control was expressed in Flp-In T-REx 293 cells. Accumulation of porphyrins in each cell line was visualized by ultraviolet light exposure (upper panel). Expression levels of each FLAG-tagged protein and GAPDH (loading control) were detected by Western blot analysis (middle panels). Expression level of ALAS2 messenger RNA (mRNA) was measured by real-time PCR, and it was normalized with the expression level of GAPDH mRNA. Note that the data confirm the similar mRNA level of each ALAS2 protein (lower panel).

unable to determine the defect of the Arg572His mutant using an in vitro system because the mutant protein showed the enzymatic activity similar to that of wild-type ALAS2.

Measurement of enzymatic activity of every recombinant protein in vitro is one of the most useful techniques to characterize a mutant ALAS2 protein. Met567Ile mutant showed lower enzymatic activity than did wild-type protein (see Fig. 2), suggesting that this mutation causes sideroblastic anemia. In contrast, we were unable to uncover the pathogenesis of Val562Ala mutant protein using this in vitro assay system, indicating a limitation of the in vitro assay system with a bacterially expressed recombinant protein. In fact, using the in vivo system (Fig. 2), we have successfully demonstrated that the Val562Ala mutant protein showed lower porphyrin accumulation due to enzyme instability compared to wild-type ALAS2. In addition, the half-life of mature Val562Ala protein (5.3 hours) was shorter than that of wild-type ALAS2 (7.8 hours) (Fig. 1), suggesting that Val562Ala mutation altered the protein stability in mitochondria. These in vivo methods seem to be useful to characterize a mutant protein that does not show decreased enzyme activity in the in vitro assay system.

It is of particular interest that the Val562Ala and Met567Ile mutants exerted opposite effects on the enzymatic activity in vitro (Table 1) and on the protein stability in mitochondria (Fig. 1). In this connection, the deletion of 33 amino acids at C-terminal end of ALAS2 protein, the region of which contains Val562 and Met567 residues, resulted in higher enzymatic activity in vitro and in vivo (Table 1) and stable protein with a longer half-life in mitochondria (Fig. 1). The C-terminal region has a suppressive function on enzymatic activity, as well as protein stability in mitochondria. Because this region is conserved in eukaryotic ALAS2 but is absent in prokaryotic ALAS, the suppressor domain might be involved in the functional regulation of ALAS2 in mitochondria. In fact, in the C-terminal region, two frame-shift mutations of the ALAS2 gene were reported to cause X-linked dominant protoporphyria [11], and six (including present two cases) missense mutations were identified in patients with XLSA. In addition, it was recently reported that the Tyr586Phe mutation of ALAS2 protein increased the enzymatic activity, which can contribute to the severe clinical phenotype of the patient with congenital erythropoietic porphyria [18]. These results suggest that the C-terminal region of ALAS2 functions as an intrinsic suppressor for protoporpyrin production in erythroid cells.

It is still unclear how this C-terminal region suppresses the enzymatic activity of ALAS2 protein in mitochondria. It has been reported that certain amino acids are essential for catalytic activity of mouse Alas2 [18,37–45]. However, only limited information is available concerning the role of the C-terminal region in the catalytic activity of ALAS2. To-Figueras et al. [18] performed the stoichiometric analysis of the mature ALAS2 protein to characterize Tyr586-Phe mutant, which was reported as a gain-of-function

mutation at the penultimate C-terminal amino acid of ALAS2 protein. Steady-state kinetic analyses revealed that Tyr586Phe mutant showed higher catalytic activity with greater catalytic efficiency for glycine and succinyl-CoA than those of wild-type ALAS2. In addition, these authors provided evidence that the Tyr586Phe mutant enzyme was able to form and release ALA more rapidly than wild-type enzyme. Similar mechanisms might underlie the increased activity of every C-terminal deletion mutant, including the mutant ALAS2 protein with the deletion of 19 or 21 amino acids [11] and the delC33 mutant. In addition, the delC33 mutant expressed enzymatic activity similar to wild-type ALAS2 without PLP in assay mixture, but its enzymatic activity was increased about twofold compared to the wild-type with PLP (Table 1). These results suggest that this region might be involved in efficient use of PLP or accessibility of PLP to the catalytic site.

Crystal structure analysis of homodimeric ALAS from Rhodobactor capsulatus ($ALAS_{RC}$) revealed that $ALAS_{RC}$ showed open or closed structure, which was related to the conformational change of the active site loop [17]. This active site loop consists of evolutionally conserved structure at the C-terminal region of $ALAS_{RC}$, and seems to cover the catalytic site, which is located at the homodimer interface of ALAS protein. It should be noted that $ALAS_{Rc}$ does not contain the C-terminal region equivalent to that of mammalian ALAS2 [17]. The open conformation was observed only in the substrate-free $ALAS_{RC}$ protein, and the closed conformation was observed in $ALAS_{RC}$ protein that bound glycine and succinyl-CoA. To clarify the functional consequence of the conformational change of this active site loop, Lendrihas et al. introduced a mutation into nonconserved amino acid at this active site loop in mouse Alas2 protein and obtained several hyperactive variants [46]. Pre–steady-state kinetic analysis revealed that release of ALA from the catalytic site of the enzyme, which is coincident with opening of the active site loop [45], was accelerated in these hyperactive variants. Because the release of ALA from catalytic site is the rate-limiting step of enzymatic reaction of ALAS [47], these results suggest that the dynamic conformational change of this active site loop might control the rate of the reaction. Importantly, the accelerated release of ALA from the enzyme was also proposed in Tyr586Phe mutant [18]. It is therefore possible that the C-terminal domain of human ALAS2 protein is involved in the regulation of the conformational change of the active site loop.

In the present study, we determined the stability of ALAS2 protein in vivo, although the protein was tagged with a small peptide and expressed in HEK293-derived cells. Based on our assay condition, the half-life of human ALAS2 mature protein is 7.8 hours; however, it is not clear whether this result is comparable with that of the native ALAS2 protein in erythroid mitochondria, which has never been reported. On the other hand, this assay revealed that the stability of the Val562Ala mutant protein was decreased in mitochondria (Fig. 1), although the in vitro assay using purified recombinant protein failed to detect the unstable property of this mutant. In addition, our in vivo assay system clearly showed that the C-terminal region of 33 amino acids of human ALAS2 protein suppressed the enzymatic activity and decreased the protein stability. It is also interesting that the Val562Ala mutation and the Met567Ile mutation have opposite effects on the two functions of the C-terminal region. These results suggest that independent mechanisms might be involved in the reduction of enzymatic activity and destabilization in mitochondria. Taken together, the C-terminal region of ALAS2 protein can decrease catalytic activity by altering the open or closed structure of the catalytic site, while the post-translational modification of the C-terminal region, which is induced by a certain intracellular condition (e.g., increased or decreased oxidative stress) or by the association with other molecules, can enhance the disappearance of ALAS2 protein from mitochondria. The crystal structure of ALAS from $ALAS_{RC}$ provided critical information about the mechanisms for catalytic reaction of ALAS [45,46]. However, determination of the crystal structure of mammalian ALAS2 should await additional investigation on the function of the C-terminal region of ALAS2 protein.

Funding disclosure

This work was supported in part by a Grant-in-Aid for Scientific Research (C) (to K. Furuyama) and Health and Labour Sciences Research Grants (to H. Harigae).

Acknowledgment

We are also grateful to Biomedical Research Core of Tohoku University Graduate School of Medicine for allowing us to use various facilities.

Conflict of interest disclosure

No financial interest/relationships with financial interest relating to the topic of this article have been declared.

References

1. Anderson KE, Sassa S, Bishop DF, Desnick RJ. Disorders of heme biosynthesis: X-linked sideroblastic anemia and the porphyrias. In: Scriver CR, Beaudet AL, Sly WS, Valle D, eds. The Metabolic & Molecular Bases of Inherited Disease. New York: McGraw-Hill Medical Publishing Division; 2001. p. 2991–3062.
2. Hayashi N, Yoda B, Kikuchi G. Difference in molecular sizes of delta-aminolevulinate synthetases in the soluble and mitochondrial fractions of rat liver. J Biochem. 1970;67:859–861.
3. Bishop DF, Henderson AS, Astrin KH. Human delta-aminolevulinate synthase: assignment of the housekeeping gene to 3p21 and the erythroid-specific gene to the X chromosome. Genomics. 1990;7: 207–214.

4. Lathrop JT, Timko MP. Regulation by heme of mitochondrial protein transport through a conserved amino acid motif. Science. 1993;259: 522–525.
5. Munakata H, Sun JY, Yoshida K, et al. Role of the heme regulatory motif in the heme-mediated inhibition of mitochondrial import of 5-aminolevulinate synthase. J Biochem. 2004;136:233–238.
6. Dailey TA, Woodruff JH, Dailey HA. Examination of mitochondrial protein targeting of haem synthetic enzymes: in vivo identification of three functional haem-responsive motifs in 5-aminolaevulinate synthase. Biochem J. 2005;386:381–386.
7. Munakata H, Yamagami T, Nagai T, Yamamoto M, Hayashi N. Purification and structure of rat erythroid-specific delta-aminolevulinate synthase. J Biochem. 1993;114:103–111.
8. Cox TC, Bawden MJ, Abraham NG, et al. Erythroid 5-aminolevulinate synthase is located on the X chromosome. Am J Hum Genet. 1990;46:107–111.
9. Cox TC, Bottomley SS, Wiley JS, Bawden MJ, Matthews CS, May BK. X-linked pyridoxine-responsive sideroblastic anemia due to a Thr388-to-Ser substitution in erythroid 5-aminolevulinate synthase. N Engl J Med. 1994;330:675–679.
10. Cotter PD, Baumann M, Bishop DF. Enzymatic defect in "X-linked" sideroblastic anemia: molecular evidence for erythroid delta-aminolevulinate synthase deficiency. Proc Natl Acad Sci U S A. 1992;89:4028–4032.
11. Whatley SD, Ducamp S, Gouya L, et al. C-terminal deletions in the ALAS2 gene lead to gain of function and cause X-linked dominant protoporphyria without anemia or iron overload. Am J Hum Genet. 2008;83:408–414.
12. Bottomley SS. Sideroblastic anemias. In: Greer JP, Foerster J, Rogers GM, et al., eds. Wintrobe's Clinical Hematology. 12th ed. Philadelphia/London: Wolters Kluwer Health/Lippincott Williams & Wilkins; 2009. p. 835–856.
13. Harigae H, Furuyama K. Hereditary sideroblastic anemia: pathophysiology and gene mutations. Int J Hematol. 2010;92:425–431.
14. Ducamp S, Kannengiesser C, Touati M, et al. Sideroblastic anemia: molecular analysis of the ALAS2 gene in a series of 29 probands and functional studies of 10 missense mutations. Hum Mutat. 2011; 32:590–597.
15. Harigae H, Furuyama K, Kimura A, et al. A novel mutation of the erythroid-specific delta-aminolaevulinate synthase gene in a patient with X-linked sideroblastic anaemia. Br J Haematol. 1999;106:175–177.
16. Cazzola M, May A, Bergamaschi G, Cerani P, Ferrillo S, Bishop DF. Absent phenotypic expression of X-linked sideroblastic anemia in one of 2 brothers with a novel ALAS2 mutation. Blood. 2002;100: 4236–4238.
17. Astner I, Schulze JO, van den Heuvel J, Jahn D, Schubert WD, Heinz DW. Crystal structure of 5-aminolevulinate synthase, the first enzyme of heme biosynthesis, and its link to XLSA in humans. EMBO J. 2005; 24:3166–3177.
18. To-Figueras J, Ducamp S, Clayton J, et al. ALAS2 acts as a modifier gene in patients with congenital erythropoietic porphyria. Blood. 2011;118:1443–1451.
19. Sambrook J, Russell DW. Molecular Cloning: A Laboratory Manual. 3rd ed. Cold Spring Harbor, NY: Cold Spring Harbor Laboratory Press; 2001.
20. Furuyama K, Fujita H, Nagai T, et al. Pyridoxine refractory X-linked sideroblastic anemia caused by a point mutation in the erythroid 5-aminolevulinate synthase gene. Blood. 1997;90:822–830.
21. Furuyama K, Harigae H, Heller T, et al. Arg452 substitution of the erythroid-specific 5-aminolaevulinate synthase, a hot spot mutation in X-linked sideroblastic anaemia, does not itself affect enzyme activity. Eur J Haematol. 2006;76:33–41.
22. Furuyama K, Sassa S. Interaction between succinyl CoA synthetase and the heme-biosynthetic enzyme ALAS-E is disrupted in sideroblastic anemia. J Clin Invest. 2000;105:757–764.
23. Kaneko K, Furuyama K, Aburatani H, Shibahara S. Hypoxia induces erythroid-specific 5-aminolevulinate synthase expression in human erythroid cells through transforming growth factor-beta signaling. FEBS J. 2009;276:1370–1382.
24. Guernsey DL, Jiang H, Campagna DR, et al. Mutations in mitochondrial carrier family gene SLC25A38 cause nonsyndromic autosomal recessive congenital sideroblastic anemia. Nat Genet. 2009;41:651–653.
25. Ye H, Jeong SY, Ghosh MC, et al. Glutaredoxin 5 deficiency causes sideroblastic anemia by specifically impairing heme biosynthesis and depleting cytosolic iron in human erythroblasts. J Clin Invest. 2010;120:1749–1761.
26. Allikmets R, Raskind WH, Hutchinson A, Schueck ND, Dean M, Koeller DM. Mutation of a putative mitochondrial iron transporter gene (ABC7) in X-linked sideroblastic anemia and ataxia (XLSA/A). Hum Mol Genet. 1999;8:743–749.
27. Bykhovskaya Y, Casas K, Mengesha E, Inbal A, Fischel-Ghodsian N. Missense mutation in pseudouridine synthase 1 (PUS1) causes mitochondrial myopathy and sideroblastic anemia (MLASA). Am J Hum Genet. 2004;74:1303–1308.
28. Ricketts CJ, Minton JA, Samuel J, et al. Thiamine-responsive megaloblastic anaemia syndrome: long-term follow-up and mutation analysis of seven families. Acta Paediatr. 2006;95:99–104.
29. Rotig A, Colonna M, Bonnefont JP, et al. Mitochondrial DNA deletion in Pearson's marrow/pancreas syndrome. Lancet. 1989;1:902–903.
30. Bergmann AK, Campagna DR, McLoughlin EM, et al. Systematic molecular genetic analysis of congenital sideroblastic anemia: evidence for genetic heterogeneity and identification of novel mutations. Pediatr Blood Cancer. 2010;54:273–278.
31. Cotter PD, Rucknagel DL, Bishop DF. X-linked sideroblastic anemia: identification of the mutation in the erythroid-specific delta-aminolevulinate synthase gene (ALAS2) in the original family described by Cooley. Blood. 1994;84:3915–3924.
32. Cotter PD, May A, Fitzsimons EJ, et al. Late-onset X-linked sideroblastic anemia. Missense mutations in the erythroid delta-aminolevulinate synthase (ALAS2) gene in two pyridoxine-responsive patients initially diagnosed with acquired refractory anemia and ringed sideroblasts. J Clin Invest. 1995;96:2090–2096.
33. Prades E, Chambon C, Dailey TA, Dailey HA, Briere J, Grandchamp B. A new mutation of the ALAS2 gene in a large family with X-linked sideroblastic anemia. Hum Genet. 1995;95:424–428.
34. Furuyama K, Uno R, Urabe A, et al. R411C mutation of the ALAS2 gene encodes a pyridoxine-responsive enzyme with low activity. Br J Haematol. 1998;103:839–841.
35. Harigae H, Furuyama K, Kudo K, et al. A novel mutation of the erythroid-specific delta-Aminolevulinate synthase gene in a patient with non-inherited pyridoxine-responsive sideroblastic anemia. Am J Hematol. 1999;62:112–114.
36. Furuyama K, Harigae H, Kinoshita C, et al. Late-onset X-linked sideroblastic anemia following hemodialysis. Blood. 2003;101: 4623–4624.
37. Ferreira GC, Neame PJ, Dailey HA. Heme biosynthesis in mammalian systems: evidence of a Schiff base linkage between the pyridoxal 5'-phosphate cofactor and a lysine residue in 5-aminolevulinate synthase. Protein Sci. 1993;2:1959–1965.
38. Gong J, Ferreira GC. Aminolevulinate synthase: functionally important residues at a glycine loop, a putative pyridoxal phosphate cofactor-binding site. Biochemistry. 1995;34:1678–1685.
39. Tan D, Ferreira GC. Active site of 5-aminolevulinate synthase resides at the subunit interface. Evidence from in vivo heterodimer formation. Biochemistry. 1996;35:8934–8941.
40. Gong J, Hunter GA, Ferreira GC. Aspartate-279 in aminolevulinate synthase affects enzyme catalysis through enhancing the function of the pyridoxal 5'-phosphate cofactor. Biochemistry. 1998;37:3509–3517.
41. Tan D, Barber MJ, Ferreira GC. The role of tyrosine 121 in cofactor binding of 5-aminolevulinate synthase. Protein Sci. 1998;7:1208–1213.

42. Tan D, Harrison T, Hunter GA, Ferreira GC. Role of arginine 439 in substrate binding of 5-aminolevulinate synthase. Biochemistry. 1998; 37:1478–1484.
43. Turbeville TD, Zhang J, Hunter GA, Ferreira GC. Histidine 282 in 5-aminolevulinate synthase affects substrate binding and catalysis. Biochemistry. 2007;46:5972–5981.
44. Lendrihas T, Zhang J, Hunter GA, Ferreira GC. Arg-85 and Thr-430 in murine 5-aminolevulinate synthase coordinate acyl-CoA-binding and contribute to substrate specificity. Protein Sci. 2009;18:1847–1859.
45. Lendrihas T, Hunter GA, Ferreira GC. Serine 254 enhances an induced fit mechanism in murine 5-aminolevulinate synthase. J Biol Chem. 2010;285:3351–3359.
46. Lendrihas T, Hunter GA, Ferreira GC. Targeting the active site gate to yield hyperactive variants of 5-aminolevulinate synthase. J Biol Chem. 2010;285:13704–13711.
47. Zhang J, Ferreira GC. Transient state kinetic investigation of 5-aminolevulinate synthase reaction mechanism. J Biol Chem. 2002;277: 44660–44669.

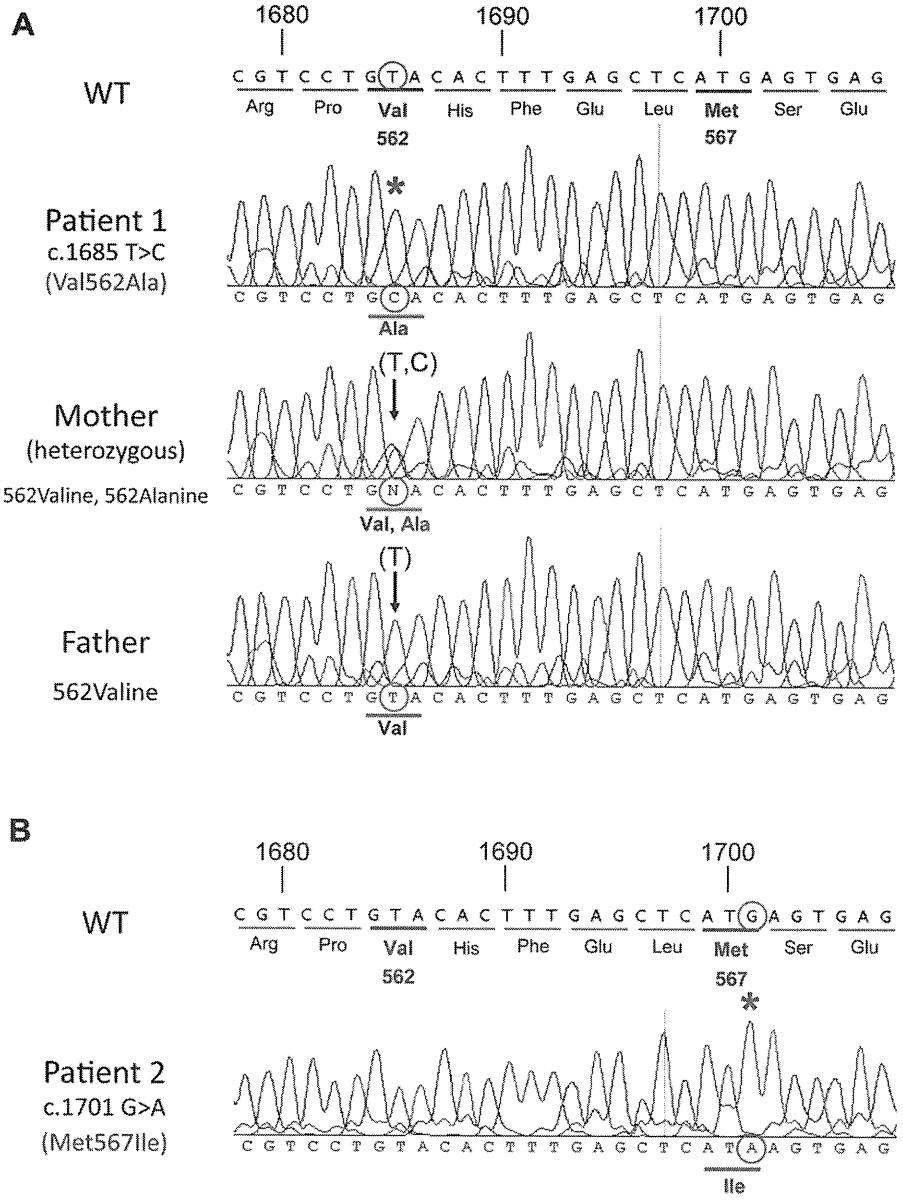

Supplementary Figure E1. Direct sequencing of 11th exon of ALAS2 gene in patients with sideroblastic anemia. Exon 11 of ALAS2 gene from each proband was amplified by PCR, and the amplicon was sequenced directly. Numbers shown at top indicate the positions of cDNA sequence, which is started from the first nucleotide of the ATG-translation initiation codon. Second and third lines indicate wild-type DNA sequence and amino acid sequence, respectively. Identified mutations are indicated with asterisks, and the expected amino acid substitution is shown under each mutation. (**A**) The c.1685T > C mutation of ALAS2 gene in case 1. The heterozygous condition of proband's mother and the wild-type allele of proband's father are shown. (**B**) The c.1701G > A mutation of ALAS2 gene in case 2.

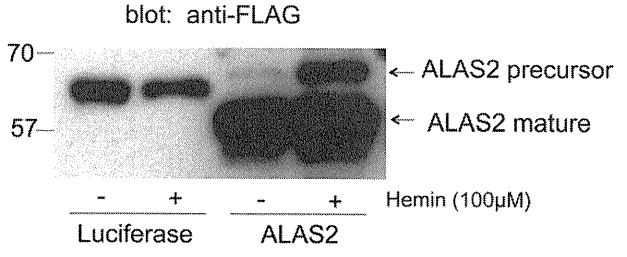

Supplementary Figure E2. Transient expression of FLAG-ALAS2 and FLAG-Luciferase in HeLa cells. HeLa human cervical cancer cells were transfected with FLAG-ALAS2 or FLAG-luciferase expression vector, then treated with 100 μM hemin. Cell lysates were subjected to the Western blot analysis with anti-FLAG antibody. Shown are the representative data.

Brief report

Identification of *TRIB1* R107L gain-of-function mutation in human acute megakaryocytic leukemia

Takashi Yokoyama,[1] Tsutomu Toki,[2] Yoshihiro Aoki,[2] Rika Kanezaki,[2] Myoung-ja Park,[3] Yohei Kanno,[1] Tomoko Takahara,[1] Yukari Yamazaki,[1] Etsuro Ito,[2] Yasuhide Hayashi,[3] and Takuro Nakamura[1]

[1]Division of Carcinogenesis, Cancer Institute, Japanese Foundation for Cancer Research, Tokyo, Japan; [2]Department of Pediatrics, Hirosaki University Graduate School of Medicine, Hirosaki, Japan; and [3]Department of Hematology/Oncology, Gunma Children's Medical Center, Gunma, Japan

Trib1 has been identified as a myeloid oncogene in a murine leukemia model. Here we identified a _TRIB1_ somatic mutation in a human case of Down syndrome–related acute megakaryocytic leukemia. The mutation was observed at well-conserved arginine 107 residue in the pseudokinase domain. This R107L mutation remained in leukocytes of the remission stage in which _GATA1_ mutation disappeared, suggesting the _TRIB1_ mutation is an earlier genetic event in leukemogenesis. The bone marrow transfer experiment showed that acute myeloid leukemia development was accelerated by transducing murine bone marrow cells with the R107L mutant in which enhancement of ERK phosphorylation and C/EBPα degradation by Trib1 expression was even greater than in those expressing wild-type. These results suggest that TRIB1 may be a novel important oncogene for Down syndrome–related acute megakaryocytic leukemia. (_Blood_. 2012; 119(11):2608-2611)

Introduction

The Down syndrome (DS) patients are predisposed to developing myeloid leukemia, and those patients frequently exhibit *GATA1* mutations.[1] However, it is proposed that the *GATA1* mutation is important for transient leukemia in DS but not sufficient for full-blown leukemia, suggesting that additional genetic alterations are needed.[1] Therefore, it is important to search the subsequent genetic changes for DS-related leukemia (ML-DS) to predict malignant transformation and prognosis of the patients.

Trib1 has been identified as a myeloid oncogene that cooperates with *Hoxa9* and *Meis1* in murine acute myeloid leukemia (AML).[2] As a member of the tribbles family of proteins, TRIB1 interacts with MEK1 and enhances ERK phosphorylation.[2,3] Moreover, TRIB1 promotes degradation of C/EBP family transcription factors, including C/EBPα, an important tumor suppressor for AML, and we observed that degradation of C/EBPα by Trib1 is mediated by its interaction with MEK1.[4] Thus, TRIB1 plays an important role in the development of AML by modulating both the RAS/MAPK pathway and C/EBPα function together with Trib2 that has also been identified as a myeloid-transforming gene.[5] Potential involvement of *TRIB1* in human leukemia has been reported in cases of AML with 8q34 amplification in which both *c-MYC* and *TRIB1* are included in the amplicon.[6] The enhancing effect of TRIB1 on the MAPK signaling suggests that TRIB1 alterations may be related to AML cases, which do not show any mutations in the pathway members, such as FLT3, c-Kit, or Ras. In this report, we identified a novel somatic mutation of *TRIB1* in a case of human acute megakaryocytic leukemia developed in DS (DS-AMKL). Retrovirus-mediated gene transfer followed by bone marrow transfer indicated that the mutation enhanced leukemogenic activity and MAPK phosphorylation by TRIB1.

Methods

Patients

TRIB1 mutations have been investigated in 12 cases of transient leukemia (TL), 5 of DS-AMKL, and 4 cell lines of DS-AML. Peripheral blood leukocytes of TL and bone marrow cells of DS-AMKL were used as sources for the molecular analysis. This study was approved by the Ethics Committee of Hirosaki University Graduate School of Medicine, and all clinical samples were obtained with informed consent from the parents of all patients, in accordance with the Declaration of Helsinki.

Patient 84 showed trisomy 21 and extensive leukocytosis at birth. Hematologic findings revealed the white blood cell count to be 148×10^9/L, including 87% myeloblasts, a hemoglobin level of 19.4 g/dL, and a platelet count of 259×10^9/L. Patent ductus arteriosus and atrial septal defect have been pointed out. Based on the hematologic data and the chromosomal abnormality, the patient was diagnosed as DS-related TL. The hematologic abnormality was then improved, but 8 months later 3% of 6.9×10^9/L white blood cells became myeloblasts (Figure 1A). A karyotype analysis of bone marrow cells revealed 48, XY,+8,+21 in 3 of 20 cells. In addition, *GATA1* mutation was detected at nt 113 from A to G, resulting in loss of the first methionine.[7] He was diagnosed as AMKL at this time, and his disease was in remission by subsequent chemotherapy.

PCR and sequencing

The entire coding region of human *TRIB1* cDNA of patients' samples was amplified using Taq polymerase (Promega) and specific primer pairs (the sequences of the primers are available on request). The genomic DNA samples of patient 84 were also analyzed. The sequence analysis of *GATA1* was performed as described previously.[7] After checking the PCR products by agarose gel electrophoresis, the products were purified and directly sequenced.

Submitted December 12, 2010; accepted January 6, 2012. Prepublished online as *Blood* First Edition paper, January 31, 2012; DOI 10.1182/blood-2010-12-324806.

The online version of this article contains a data supplement.

The publication costs of this article were defrayed in part by page charge payment. Therefore, and solely to indicate this fact, this article is hereby marked "advertisement" in accordance with 18 USC section 1734.

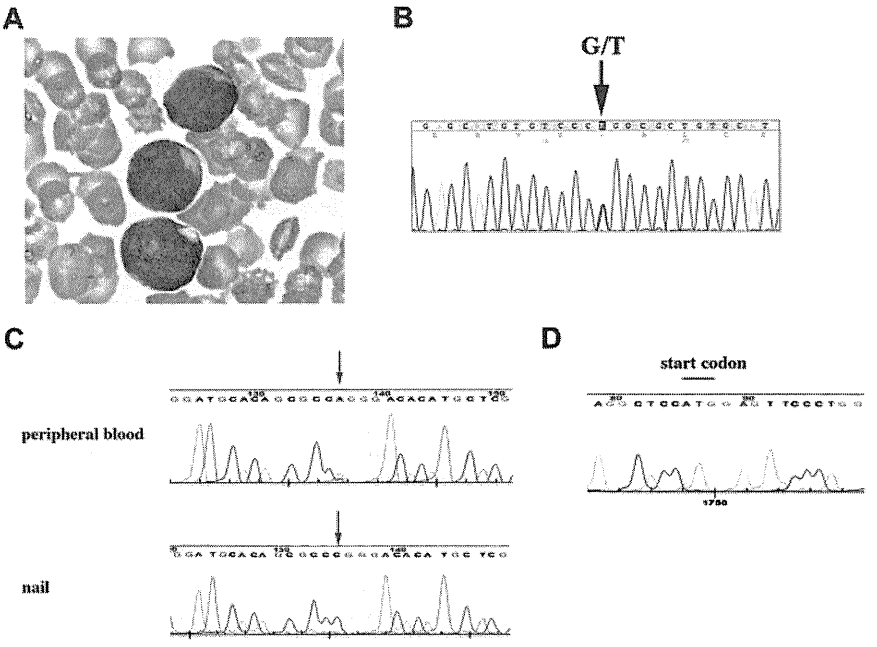

Figure 1. *TRIB1* R107L mutation identified in DS-related leukemias. (A) Giemsa staining of the case 84 peripheral blood smear diagnosed as AMKL. The image was acquired using a BX40 microscope equipped with a 100×/1.30 NA oil objective (Olympus) and a C-4040 digital camera (Olympus). (B) Fluorescent dye sequencing chromatographs of *TRIB1* genotyping by direct sequencing of the case 84 using a cDNA sample as a template. The vertical arrow indicates mixed G and T signals at codon 107. (C) Fluorescent dye sequencing chromatographs of *TRIB1* of peripheral blood leukocytes (top) or nail (bottom) in the same case at the complete remission stage. The red arrows indicate that the mutation remains in leukocytes but not in nail. The reverse strand sequences are shown. (D) *GATA1* sequence. The start codon that was mutated in AMKL[7] is normal in the peripheral blood leukocytes at the remission stage.

Retroviral infection of murine bone marrow cells and bone marrow transfer

Bone marrow cells were prepared from 8-week-old female C57Bl/6J mice 5 days after injection of 150 mg/kg body weight of 5-fluorouracil (Kyowa Hakko Kogyo). Retroviral infection of bone marrow cells and bone marrow transfer experiments were performed as described.[2] Transduction efficiencies evaluated by flow cytometric techniques were comparable between wild-type (WT; 5.3%) and R107L (3.4%). Animals were housed, observed daily, and handled in accordance with the guidelines of the animal care committee at Japanese Foundation for Cancer Research. All the diseased mice were subjected to autopsy and analyzed morphologically, and the blood was examined by flow cytometric techniques. The mice were diagnosed as positive for AML according to the classification of the Bethesda proposal.[8] The survival rate of each group was evaluated using the Kaplan-Meier method, and differences between survival curves were compared using the log-rank test.

Immunoblotting

Immunoblotting was performed using cell lysates in RIPA buffer as described.[4] Anti-p44/42 ERK (Cell Signaling Technologies), anti–phospho-p44/42 ERK (Cell Signaling Technologies), anti-C/EBPα (Santa Cruz Biotechnology), anti-FLAG (Sigma-Aldrich), and anti-GAPDH (Hy Test Ltd) antibodies were used.

Results and discussion

The important role of TRIB1 on the MAPK signaling suggests that *TRIB1* alterations may occur in some AML cases, which do not show overlapping mutations in the pathway members, such as FLT3, KIT, or RAS. Therefore, we tried to search mutations of *TRIB1* in cases of ML-DS and TL in which such mutations are infrequent.[9] In a case of DS-AMKL (case 84), a nucleotide change from guanine to thymine has been identified at 902 that results in amino acid alteration from arginine 107 (R107) to leucine (Figure 1B). The sequence changes were confirmed by subcloning the PCR product into the TA-type plasmid vector (data not shown). The nucleotide change was not observed in the DNA sample derived from the nail of the same patient at all (Figure 1C), indicating that this change is a somatic mutation. Interestingly, the mutation was retained in the peripheral blood sample in the complete remission stage in which the GATA1 mutation completely disappeared (Figure 1C-D). These results indicate that the *TRIB1* mutation precedes the onset of TL and the *GATA1* mutation, and suggest that *TRIB1* mutation occurred at the hematopoietic stem cell level and that the clone retaining the *TRIB1* mutation survived after chemotherapy. In case 84, there was no mutation for *FLT3* exons 14, 15, and 20, *PTPN11* exons 3 and 13, *KRAS* exons 2, 3, and 5, and *KIT* exons 8, 11, and 17 by the high-resolution melt analysis (data not shown).

An additional mutation was found in a case of TL (case 109) at the nucleotides 805 and 806 from GC to AT, which results in amino acid conversion from alanine (A75) to isoleucine (supplemental Figure 1, available on the *Blood* Web site; see the Supplemental Materials link at the top of the online article). *TRIB1* expression in DS-related and DS-unrelated leukemias was examined by real-time quantitative RT-PCR (supplemental Figure 2).

R107 is located within a psuedokinase domain of TRIB1 that is considered as a functionally core domain of TRIB family proteins.[10] Sequence comparison among 3 TRIB family proteins as well as tribbles homologs in other organisms revealed that the R107 is well conserved in mammalian TRIB1 and TRIB2,[10] suggesting that this arginine residue is evolutionary conserved and may be related to an important function. On the other hand, A75 is located outside of the pseudokinase domain, not conserved between human and mouse, or other tribbles homologs. Moreover, the N-terminal domain containing A75 is dispensable for the leukemogenic activity of Trib1.[4] Therefore, we tried to investigate whether the R107L mutation could affect the leukemogenic activity of *TRIB1*.

R107L was introduced into the murine *Trib1* cDNA by site-directed mutagenesis. Both WT and R107L cDNAs were subcloned into the pMYs-IRES-GFP retroviral vector and were used for retrovirus-mediated gene transfer followed by bone marrow transfer according to the method previously described.[1] All the mice

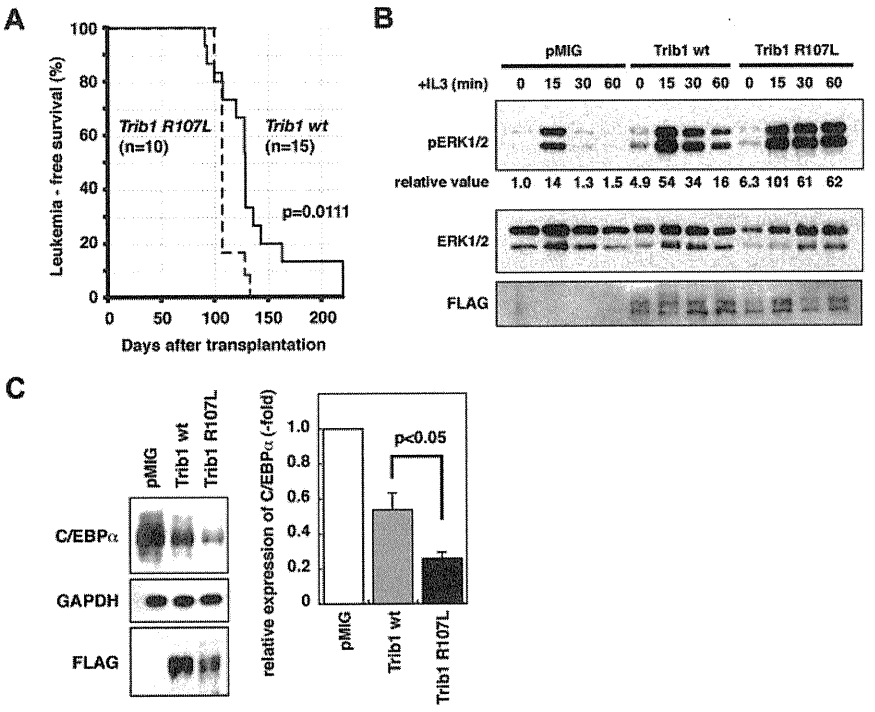

Figure 2. AML development by bone marrow transfer using *Trib1* WT and R107L. (A) Kaplan-Meier survival curves are shown. The *P* value was calculated with the log-rank test. (B) Immunoblot analysis of *Trib1* WT AML (Mac-1 56.2%, Gr-1 52.5%, $CD34^{lo}$, c-kit^{-}, Sca-1^{-}) and R107L AML (Mac-1 41.4%, Gr-1 25.2%, $Cd34^{lo}$, c-kit^{lo}, Sca-1^{-}) derived from bone marrow of recipient mice (WT #T73 and R107L #T151 in supplemental Table 1). Enhancement of ERK phosphorylation is more significant in R107L. Relative values of ERK phosphorylation were calculated by densitometric analysis. (C) Immunoblot analysis for C/EBPα of the same AML samples as in panel B. Relative expression level of C/EBPα is quantitated (right).

transplanted with bone marrow cells expressing WT (n = 15) or R107L (n = 12) developed AML (Figure 2A). The mean survival time was shorter in the recipients with R107L-expressing bone marrow cells (110 days) than those with WT (136 days; Figure 2A). The difference was significant ($P = .0111$, log-rank test). The result indicates that the R107L mutation enhances the leukemogenic activity of TRIB1. These results also suggest that *TRIB1* mutation might cooperate with *GATA1* mutation in the genesis of DS-AMKL, and that trisomy 21, *TRIB1*, and *GATA1* mutations occurred consecutively, which contributed to the multistep leukemogenic process.

We have shown that TRIB1 interacts with MEK1 and enhances phosphorylation of ERK.[2] The R107L mutant enhanced ERK phosphorylation more extensively than WT (Figure 2B) in AML cells derived from bone marrow of recipient mice, and more significant degradation of C/EBPα was induced by the R107L mutant (Figure 2C). These findings might be correlated to the enhanced leukemogenic activity of the mutant. Both R107L and WT proteins could interact with MEK1, having the binding motif in their C-termini. The residue 107 is located at subdomain II of the pseudokinase domain.[11] The mutation may affect conformation of the domain and may promote the MEK1 function on ERK, although additional studies are required to address the possibility. A recent study demonstrates that Trib1 and Trib2 failed to show ERK phosphorylation in 32D cells.[12] The different response to Trib1 between primary leukemic cells and the cell line might depend on the cellular context and/or combination of additional mutations. The AML phenotypes were somewhat varied in each case and Mac-1–positive/Gr-1–negative AMLs were more remarkable in WT than in R107L, although the difference was not statistically significant (supplemental Figures 3-4; supplemental Table 1). The current study underscores the role of TRIB1 in human leukemogenesis and the significance of the R107L mutation in its function. Further sequence analysis of tribbles family genes in a larger cohort will emphasize the importance of R107L and/or additional mutations of *TRIB1* in leukemic patients.

Acknowledgments

This work was supported by KAKENHI (Grant-in-Aid for Scientific Research) on Priority Areas Integrative Research Toward the Conquest of Cancer (E.I. and T.N.) and the Ministry of Education, Culture, Sports, Science and Technology of Japan (Young Scientists, T.Y.).

Authorship

Contribution: T.Y., E.I., Y.H., and T.N. designed and performed the research and wrote the manuscript; T. Toki, Y.A., R.K., and M.-j.P. performed the research; and Y.K., T. Takahara, and Y.Y. contributed to the bone marrow transplantation analysis.

Conflict-of-interest disclosure: The authors declare no competing financial interests.

Correspondence: Takuro Nakamura, Division of Carcinogenesis, Cancer Institute, Japanese Foundation for Cancer Research, 3-8-31 Ariake, Koto-ku, Tokyo 135-8550, Japan; e-mail: takuro-ind@umin.net.

References

1. Shimizu R, Engel JD, Yamamoto M. GATA1-related leukaemias. *Nat Rev Cancer.* 2008;8(4):279-287.
2. Jin G, Yamazaki Y, Takuwa M, et al. Trib1 and Evi1 cooperate with Hoxa and Meis1 in myeloid leukemogenesis. *Blood.* 2007;109(9):3998-4005.
3. Kiss-Toth E, Bagstaff SM, Sung HY, et al. Human Tribbles, a protein family controlling mitogen-activated protein kinase cascades. *J Biol Chem.* 2004;279(41):42703-42708.
4. Yokoyama T, Kanno Y, Yamazaki Y, et al. Trib1 links the MEK/ERK pathway in myeloid

leukemogenesis. *Blood.* 2010;116(15):2768-2775.

5. Keeshan K, He Y, Wouters BJ, et al. Tribbles homolog 2 inactivates C/EBPalpha and causes acute myelogenous leukemia. *Cancer Cell.* 2006; 10(5):401-411.
6. Storlazzi CT, Fioretos T, Surace C, et al. MYC-containing double minutes in hematologic malignancies: evidence in favor of the episome model and exclusion of MYC as the target gene. *Hum Mol Genet.* 2006;15(6):933-942.
7. Kanezaki R, Toki T, Terui K, et al. Down syndrome and GATA1 mutations in transient abnormal myeloproliferative disorder: mutation classes correlate with progression to myeloid leukemia. *Blood.* 2010;116(22):4631-4638.
8. Kogan SC, Ward JM, Anver MR, et al. Bethesda proposal for classification of nonlymphoid hematopoietic neoplasms in mice. *Blood.* 2002;100(1): 238-245.
9. Toki T, Kanezaki R, Adachi S, et al. The key role of stem cell factor/KIT signaling in the proliferation of blast cells from Down syndrome-related leukemia. *Leukemia.* 2009;23(1):95-103.
10. Hegedus Z, Czibula A, Kiss-Toth E. Tribbles: a family of kinase-like proteins with potent signaling regulatory function. *Cell Signal.* 2007;19(2):238-250.
11. Yokoyama T, Nakamura T. Tribbles in disease: signaling pathways important for cellular function and neoplastic transformation. *Cancer Sci.* 2011;102(6):1115-1122.
12. Dedhia PH, Keeshan K, Uljon S, et al. Differential ability of Tribbles family members to promote degradation of C/EBPalpha and induce acute myelogenous leukemia. *Blood.* 2010; 116(8):1321-1328.

Extensive gene deletions in Japanese patients with Diamond-Blackfan anemia

Madoka Kuramitsu,[1] Aiko Sato-Otsubo,[2] Tomohiro Morio,[3] Masatoshi Takagi,[3] Tsutomu Toki,[4] Kiminori Terui,[4] RuNan Wang,[4] Hitoshi Kanno,[5] Shouichi Ohga,[6] Akira Ohara,[7] Seiji Kojima,[8] Toshiyuki Kitoh,[9] Kumiko Goi,[10] Kazuko Kudo,[11] Tadashi Matsubayashi,[12] Nobuo Mizue,[13] Michio Ozeki,[14] Atsuko Masumi,[1] Haruka Momose,[1] Kazuya Takizawa,[1] Takuo Mizukami,[1] Kazunari Yamaguchi,[1] Seishi Ogawa,[2] Etsuro Ito,[4] and Isao Hamaguchi[1]

[1]Department of Safety Research on Blood and Biological Products, National Institute of Infectious Diseases, Tokyo, Japan; [2]Cancer Genomics Project, Graduate School of Medicine, The University of Tokyo, Tokyo, Japan; [3]Department of Pediatrics and Developmental Biology, Graduate School of Medicine, Tokyo Medical and Dental University, Bunkyo-ku, Tokyo, Japan; [4]Department of Pediatrics, Hirosaki University Graduate School of Medicine, Hirosaki, Japan; [5]Department of Transfusion Medicine and Cell Processing, Tokyo Women's Medical University, Tokyo, Japan; [6]Department of Pediatrics, Graduate School of Medical Sciences, Kyushu University, Fukuoka, Japan; [7]First Department of Pediatrics, Toho University School of Medicine, Tokyo, Japan; [8]Department of Pediatrics, Nagoya University Graduate School of Medicine, Nagoya, Japan; [9]Department of Hematology/Oncology, Shiga Medical Center for Children, Shiga, Japan; [10]Department of Pediatrics, School of Medicine, University of Yamanashi, Yamanashi, Japan; [11]Division of Hematology and Oncology, Shizuoka Children's Hospital, Shizuoka, Japan; [12]Department of Pediatrics, Seirei Hamamatsu General Hospital, Shizuoka, Japan; [13]Department of Pediatrics, Kushiro City General Hospital, Hokkaido, Japan; and [14]Department of Pediatrics, Graduate School of Medicine, Gifu University, Gifu, Japan

Fifty percent of Diamond-Blackfan anemia (DBA) patients possess mutations in genes coding for ribosomal proteins (RPs). To identify new mutations, we investigated large deletions in the RP genes *RPL5*, *RPL11*, *RPL35A*, *RPS7*, *RPS10*, *RPS17*, *RPS19*, *RPS24*, and *RPS26*. We developed an easy method based on quantitative-PCR in which the threshold cycle correlates to gene copy number. Using this approach, we were able to diagnose 7 of 27 Japanese patients (25.9%) possessing mutations that were not detected by sequencing. Among these large deletions, similar results were obtained with 6 of 7 patients screened with a single nucleotide polymorphism array. We found an extensive intragenic deletion in *RPS19*, including exons 1-3. We also found 1 proband with an *RPL5* deletion, 1 patient with an *RPL35A* deletion, 3 with *RPS17* deletions, and 1 with an *RPS19* deletion. In particular, the large deletions in the *RPL5* and *RPS17* alleles are novel. All patients with a large deletion had a growth retardation phenotype. Our data suggest that large deletions in RP genes comprise a sizable fraction of DBA patients in Japan. In addition, our novel approach may become a useful tool for screening gene copy numbers of known DBA genes. (*Blood*. 2012;119(10): 2376-2384)

Introduction

Diamond-Blackfan anemia (DBA; MIN# 105650) is a rare congenital anemia that belongs to the inherited BM failure syndromes, generally presenting in the first year of life. Patients typically present with a decreased number of erythroid progenitors in their BM.[1] A main feature of the disease is red cell aplasia, but approximately half of patients show growth retardation and congenital malformations in the craniofacial, upper limb, cardiac, and urinary systems. Predisposition to cancer, in particular acute myeloid leukemia and osteogenic sarcoma, is also characteristic of the disease.[2]

Mutations in the *RPS19* gene were first reported in 25% of DBA patients by Draptchinskaia et al in 1999.[3] Since that initial finding, many genes that encode large (RPL) or small (RPS) ribosomal subunit proteins were found to be mutated in DBA patients, including *RPL5* (approximately 21%), *RPL11* (approximately 9.3%), *RPL35A* (3.5%), *RPS7* (1%), *RPS10* (6.4%), *RPS17* (1%), *RPS24* (2%), and *RPS26* (2.6%).[4-7] To date, approximately half of the DBA patients analyzed have had a mutation in one of these genes. Konno et al screened 49 Japanese patients and found that 30% (12 of 49) carried mutations.[8] In addition, our data showed that 22 of 68 DBA patients (32.4%) harbored a mutation in ribosomal protein (RP) genes (T.T., K.T., R.W., and E.I., unpublished observation, April 16, 2011). These abnormalities of RP genes cause defects in ribosomal RNA processing, formation of either the large or small ribosome subunit, and decreased levels of polysome formation,[4-6,9-12] which is thought to be one of the mechanisms for impairment of erythroid lineage differentiation.

Although sequence analyses of genes responsible for DBA are well established and have been used to identify new mutations, it is estimated that approximately half of the mutations remain to be determined. Because of the difficulty of investigating whole allele deletions, there have been few reports regarding allelic loss in DBA, and they have only been reported for *RPS19* and *RPL35A*.[3,6,13] However, a certain percentage of DBA patients are thought to have a large deletion in RP genes. Therefore, a detailed analysis of allelic loss mutations should be conducted to determine other RP genes that might be responsible for DBA.

In the present study, we investigated large deletions using our novel approach for gene copy number variation analysis based on quantitative-PCR and a single nucleotide polymorphism (SNP) array. We screened Japanese DBA patients and found 7 patients with a large deletion in an allele in *RPL5*, *RPL35A*, *RPS17*, or *RPS19*. Interestingly, all of these patients with a large deletion had a phenotype of growth retardation, including short stature and

Submitted July 24, 2011; accepted November 15, 2011. Prepublished online as *Blood* First Edition paper, January 18, 2012; DOI 10.1182/blood-2011-07-368662.

The online version of this article contains a data supplement.

The publication costs of this article were defrayed in part by page charge payment. Therefore, and solely to indicate this fact, this article is hereby marked "advertisement" in accordance with 18 USC section 1734.

Table 1. Primers used for synchronized quantitative-PCR (s-q-PCR) of RPL proteins

Gene	Primer name	Sequence	Primer name	Sequence	Size, bp
RPL5	L5-02F	CTCCCAAAGTGCTTGAGATTACAG	L5-02R	CACCTTTTCCTAACAAATTCCCAAT	132
	L5-05F	AGCCCTCCAACCTAGGTGACA	L5-05R	GAATTGGGATGGGCAAGAACT	102
	L5-17F	TGAACCCTTGCCCTAAAACATG	L5-17R	TCTTGGTCAGGCCCTGCTTA	105
	L5-19F	ATTGTGCAAACTCGATCACTAGCT	L5-19R	GTGTCTGAGGCTAACACATTTCCAT	103
	L5-21F	GTGCCACTCTCTTGGACAAACTG	L5-21R	CATAGGGCCAAAAGTCAAATAGAAG	102
	L5-28F	TCCACTTTAGGTAGGCGAAACC	L5-28R	TCAGATTTGGCATGTACCTTTCA	102
RPL11	L11-06F	GCACCCACATGGCTTAAAGG	L11-6R	CAACCAACCCATAGGCCAAA	102
	L11-20F	GAGCCCCCTTTCTCAGATGATA	L11-20R	CATGAACTTGGGCTCTGAATCC	109
	L11-22F	TATGTGCAGATAAGAGGGCAGTCT	L11-22R	ATACAGATAAGGAAACTGAGGCAGATT	98
RPL19	L19-02F	TGGCCTCTCATAAAGGAAATCTCT	L19-02R	GGAATGCAGGCAAGTTACTCTGTT	103
	L19-08F	TTTGAAGGCAAGAAATAAGTTCCA	L19-08R	AGCACATCACAGAGTCCAAATAGG	107
	L19-16F	GGTTAGTTGAAGCAGGAGCCTTT	L19-16R	TGCTAGGGAGACAGAAGCACATC	102
	L19-19F	GGACCAGTAGTTGTGACATCAGTTAAG	L19-19R	CCCATTTGTAACCCCCACTTG	106
RPL26	L26-03F	TCCAAAGAGCTGAGACAGAAGTACA	L26-03R	TCCATCAAGACAACGAGAACAAGT	102
	L26-16F	TTTGAGAATGCTTGAGAGAAGGAA	L26-16R	TTCCAGCACATGTAAAATCAAGGA	102
	L26-18F	ATGTTTTAATAAGCCCTCCAGTTGA	L26-18R	GAGAACAGCAAGTTGAAAGGTTCA	102
	L26-20F	GGGCTTTGCTTGATCACTCTAGA	L26-20R	AGGGAGCCCGAAAACATTTAC	104
RPL35A	L35A-01F	TGTGGCTTCTATTTTGCGTCAT	L35A-01R	GGAATTACCTCCTTTATTGCTTACAAG	121
	L35A-07F	TTTCCGTTCTGTCTATTGCTGTGT	L35A-07R	GAACCCTGAGTGGAGGATGTTC	113
	L35A-17F	GCCCACAACCTCCAGAGAATC	L35A-17R	GGATCACTTGAGGCCAGGAAT	104
	L35A-18F	TTAGGTGGGCTTTTCAGTCTCAA	L35A-18R	ATCTCCTGATTCCCCAACTTTGT	102
RPL36	L36-02F	CCGCTCTACAAGTGAAGAAATTCTG	L36-02R	CTCCCTCTGCCTGTGAAATGA	102
	L36-04F	TGCGTCCTGCCAGTGTTG	L36-04R	GGGTAGCTGTGAGAACCAAGGT	105
	L36-17F	CCCCTTGAAAGGACAGCAGTT	L36-17R	TTGGACACCAGGCACAGACTT	114

Table 2. Primers used for s-q-PCR of RPS proteins

Gene	Primer name	Sequence	Primer name	Sequence	Size, bps
RPS7	S7-11F	GCGCTGCCAGATAGGAAATC	S7-11R	TTAGGGAGCTGCCTTACATATGG	102
	S7-12F	ACTGGCAGTTCTGTGATGCTAAGT	S7-12R	ACTCTTGCTCATCTCCAAAACCA	102
	S7-16F	GTGTCTGTGCCAGAAAGCTTGA	S7-16R	GAACCATGCAAAAGTGCCAATAT	112
RPS10	S10-03F	CTACGGTTTTGTGTGGGTCACTT	S10-03R	CATCTGCAAGAAGGAGACGATTG	102
	S10-15F	GTTGGCCTGGAGTCGTGATTT	S10-15R	ATTCCAAGTGCACCATTTCCTT	101
	S10-17F	AATGGTGTTTAGGCCAACGTTAC	S10-17R	TTTGAACAGTGGTTTTTGTGCAT	100
RPS14	S14-03F	GAATTCCAAACCCTTCTGCAAA	S14-03R	TTGCTTCATTTACTCCTCAAGACATT	104
	S14-05F	ACAACCAGCCCTCTACCTCTTTT	S14-05R	GGAAGACGCCGGCATTATT	102
	S14-06F	CGCCTCTACCTCGCCAAAC	S14-06R	GGGATCGGTGCTATTGTTATTCC	102
	S14-09F	GCCATCATGCCGAAACATACT	S14-09R	AACGCGCCACAGGAGAGA	102
	S14-13F	ATCAGGTGGAGCACAGGAAAAC	S14-13R	GCGAGGGAGCTGCTTGATT	111
	S14-15F	AGAAGTTTTAGTGAGGCAGAAATGAGA	S14-15R	TCCCCTGGCTATTAAATGAAACC	102
	S14-19F	GATGAATTGTCCTTTCCTCCATTC	S14-19R	TAGGCGGAAACCAAAAATGCT	102
RPS15	S15-11F	CTCAGCTAATAAAGGCGCACATG	S15-11R	CCTCACACCACGAACCTGAAG	108
	S15-15F	GGTTGGAGAACATGGTGAGAACTA	S15-15R	CACATCCCTGGGCCACTCT	108
RPS17	S17-03F	ACTGCTGTCGTGGCTCGATT	S17-03R	GATGACCTGTTCTTCTGGCCTTA	121
	S17-05F	GAAAACAGATACAAATGGCATGGT	S17-05R	TGCCTCCCACTTTTCCAGAGT	114
	S17-12F	CTATGTGTAGGAGGTCCCAGGATAG	S17-12R	CCACCTGGTACTGAGCACATGT	102
	S17-16F	TAGCGGAAGTTGTGTGCATTG	S17-16R	CAAGAACAGAAGCAGCCAAGAG	102
	S17-18F	TGGCTGAATCTGCCTGCTT	S17-18R	GCCTTGTATGTACCTGGAAATGG	103
	S17-20F	GGGCCCTTCACAAATGTTGA	S17-20R	GCAAAACTCTGTCCCTTTGAGAA	101
RPS19	S19-24F	CCATCCCAAGAATGCACACA	S19-24R	CGCCGTAGCTGGTACTCATG	120
	S19-28F	GACACACCTGTTGAGTCCTCAGAGT	S19-28R	GCTTCTATTAACTGGAGCACACATCT	114
	S19-36F	CTCTTGAGGGTGGTCTGGAAAT	S19-36R	GTCTTTGCGGGTTCTTCCTCTAC	102
	S19-40F	GGAACGGTGTCAGGATTCAAG	S19-40R	AGCGGCTGTACACCAGAAATG	101
	S19-44F	CTGAGGTTGAGTGTCCCATTTCT	S19-44R	GCACCGGGCCTCTGTTATC	104
	S19-57F	CAGGGACACAGTGCTGAGAAACT	S19-57R	TGAGATGTCCCATTTTCACTATTGTT	101
	S19-58F	CATGATGTTAGCTCCGTTGCATA	S19-58R	ATTTTGGGAAGAGTGAAGCTTAGGT	102
	S19-62F	GCAACAGAGCGAGACTCCATTT	S19-62R	AGCACTTTTCGGCACTTACTTCA	102
	S19-65F	ACATTTCCCAGAGCTGACATGA	S19-65R	TCGGGACACCTAGACCTTGCT	102
RPS24	S24-17F	CGACCACGTCTGGCTTAGAGT	S24-17R	CCTTCATGCCCAACCAAGTC	101
	S24-20F	ACAAGTAAGCATCATCACCTCGAA	S24-20R	TTTCCCTCACAGCTATCGTATGG	105
	S24-32F	GGGAAATGCTGTGTCCACATACT	S24-32R	CTGGTTTCATGGCTCCAGAGA	105
RPS26	S26-03F	CGCAGCAGTCAGGGACATTT	S26-03R	AAGTTGGGCGAAGGCTTTAAG	104
	S26-05F	ATGGAGGCCGTCTAGTTTGGT	S26-05R	TGCCTACCCTGAACCTTGCT	102
RPS27A	S27A-09F	GCTGGAGTGCATTCGCTTGT	S27A-09R	CACGCCTGTAATCCCCACTAA	102
	S27A-12F	CAGGCTTGGTGTGCTGTGACT	S27A-12R	ACGTCCATCTTCCAGCTGCTT	103
	S27A-18F	GGGTTTTTCCTGTTTGGTATTTGA	S27A-18R	AAAGGCCAGCTTTGCAAGTG	111
	S27A-22F	TTACCATATTGCCAGTCTTTCCATT	S27A-22R	TTCATATGCATTTGCACAAACTGT	106

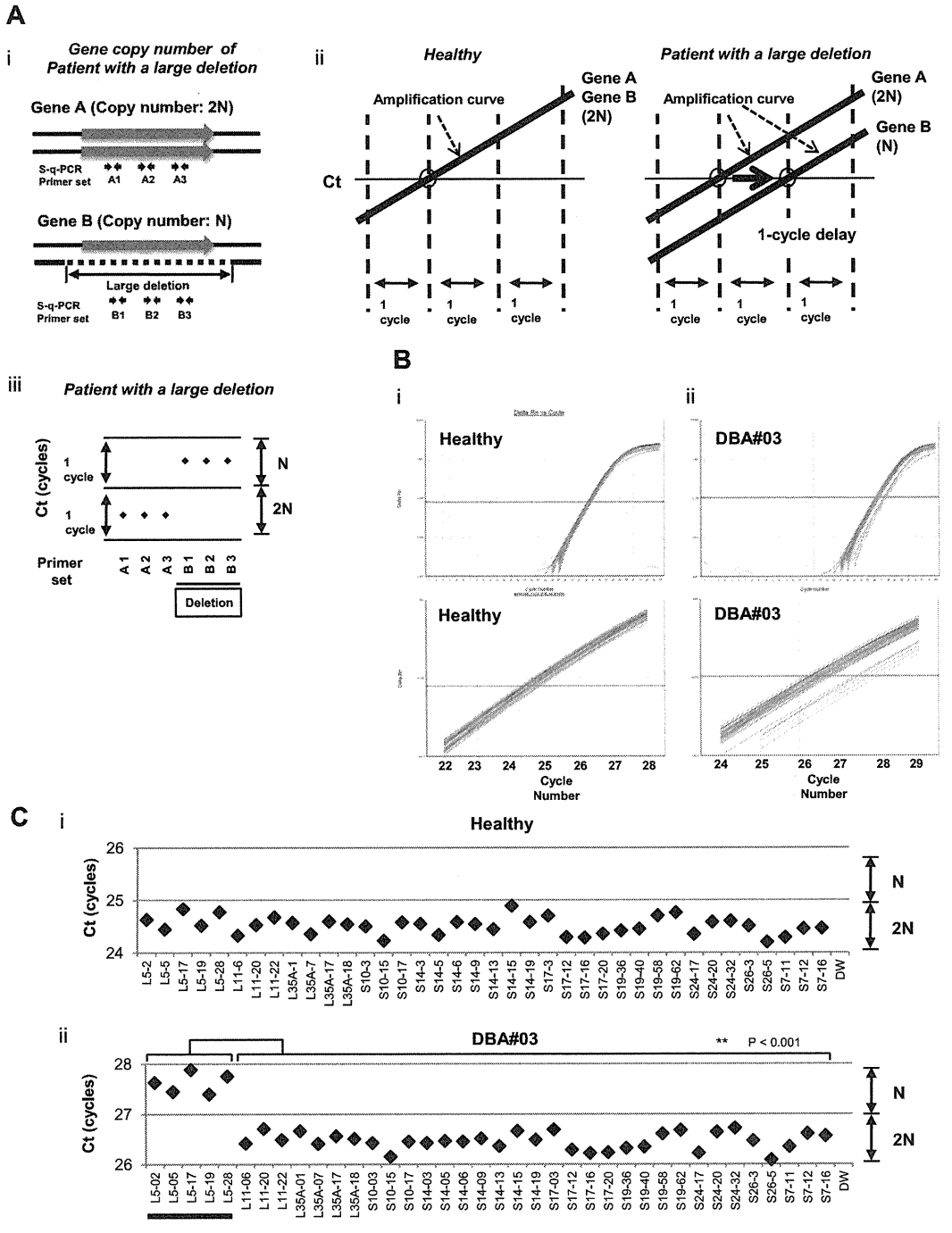

Figure 1. s-q-PCR can determine a large gene deletion in DBA. (A) Concept of the DBA s-q-PCR assay. The difference in gene copy number between a healthy sample and that with a large deletion is 2-fold (i). When all genomic s-q-PCR for genes of interest synchronously amplify DNA fragments, a 2-fold difference in the gene copy number is detected by a 1-cycle difference of the Ct scores of the s-q-PCR amplification curves (ii). Also shown is a dot plot of the Ct scores (iii). (B) Results of the amplification curves of s-q-PCR performed with a healthy person (i) and a DBA patient (patient 3; ii). The top panel shows the results of PCR cycles; the bottom panel is an extended graph of the PCR cycles at logarithmic amplification. (C) Graph showing Ct scores of s-q-PCR. If all specific primer sets for DBA genes show a 1-cycle delay relative to each other, this indicates a large deletion in the gene. Gene primer sets with a large deletion are underlined in the graph. $^{**}P < .001$.

small-for-gestational age (SGA), which suggests that this is a characteristic of DBA patients with a large gene deletion in Japan.

Methods

Patient samples

Genomic DNA was extracted using the GenElute Blood Genomic DNA Kit (Sigma-Aldrich) according to the manufacturer's protocol. Clinical manifestation of patients from a Japanese DBA genomic library are listed elsewhere or are as reported by Konno et al.[8] The study was approved by the institutional review board at the National Institute of Infectious Diseases and Hirosaki University.

DBA gene copy number assay by s-q-PCR

For s-q-PCR, primers were designed using Primer Express Version 3.0 software (Applied Biosystems). Primers are listed in Tables 1 and 2. Genomic DNA in water was denatured at 95°C for 5 minutes and

immediately cooled on ice. The composition of the s-q-PCR mixture was as follows: 5 ng of denatured genomic DNA, 0.4mM forward and reverse primers, 1× SYBR Premix Ex Taq II (Takara), and 1× ROX reference dye II (Takara) in a total volume of 20 μL (all experiments were performed in duplicate). Thermal cycling was performed using the Applied Biosystems 7500 fast real-time PCR system. Briefly, the PCR mixture was denatured at 95°C for 30 seconds, followed by 35 cycles of 95°C for 5 seconds, 60°C for 34 seconds, and then dissociation curve measurement. Threshold cycle (Ct) scores were determined as the average of duplicate samples. The technical errors of Ct scores in the triplicate analysis were within 0.2 cycles (supplemental Figure 1, available on the *Blood* Web site; see the Supplemental Materials link at the top of the online article). The sensitivity and specificity of this method was evaluated with 15 healthy samples. Any false positive was not observed in all primer sets in all healthy samples (supplemental Figure 2). We performed direct sequencing of the s-q-PCR products. The results of the sequence analysis were searched for using BLAST to confirm uniqueness. Sequence data were obtained from GenBank (http://www.ncbi.nlm.nih.gov/gene/) and Ensemble Genome Browser (http://uswest.ensembl.org).

Genomic PCR

Genomic PCR was performed using KOD FX (Toyobo) according to the manufacturer's step-down PCR protocol. Briefly, the PCR mixture contained 20 ng of genomic DNA, 0.4mM forward and reverse primers, 1mM dNTP, 1× KOD FX buffer, and 0.5 U KOD FX in a total volume of 25 μL in duplicate. Primers are given in supplemental Figure 3 and Table 2. PCR mixtures were denatured at 94°C for 2 minutes, followed by 4 cycles of 98°C for 10 seconds, 74°C for 12 minutes, followed by 4 cycles of 98°C for 10 seconds, 72°C for 12 minutes followed by 4 cycles of 98°C for 10 seconds, 70°C for 12 minutes, followed by 23 cycles of 98°C for 10 seconds and 68°C for 12 minutes. PCR products were loaded on 0.8% agarose gels and detected by LAS-3000 (Fujifilm).

DNA sequencing analysis

The genomic PCR product was purified by the GenElute PCR clean-up kit (Sigma-Aldrich) according to the manufacturer's instructions. Direct sequencing was performed using the BigDye Version 3 sequencing kit. Sequences were read and analyzed using a 3120x genetic analyzer (Applied Biosystems).

SNP array-based copy number analysis

SNP array experiments were performed according to the standard protocol of GeneChip Human Mapping 250K Nsp arrays (Affymetrix). Microarray data were analyzed for determination of the allelic-specific copy number using the CNAG program, as described previously.[14] All microarray data are available at the EGA database (www.ebi.ac.uk/ega) under accession number EGAS00000000105.

Results

Construction of a convenient method for RP gene copy number analysis based on s-q-PCR

We focused on the heterozygous large deletions in DBA-responsible gene. The difference in copy number of genes between a mutated DBA allele and the intact allele was 2-fold (N and 2N; Figure 1Ai). If each PCR can synchronously amplify DNA fragments when the template genomic DNA used is of normal karyotype, it is possible to conveniently detect a gene deletion with a 1-cycle delay in s-q-PCR analysis (Figure 1Aii-iii).

Table 3. Summary of mutations and the mutation rate observed in Japanese DBA patients

Gene	Sequencing analysis
RPS19	10
RPL5	6
RPL11	3
RPS17	1
RPS10	1
RPS26	1
RPL35A	0
RPS24	0
RPS14	0
Mutations, n (%)	22 (32.4%)
Total analyzed, N	68

To apply this strategy for allelic analysis of DBA, we prepared primers for 16 target genes, *RPL5*, *RPL11*, *RPL35A*, *RPS10*, *RPS19*, *RPS26*, *RPS7*, *RPS17*, *RPS24*, *RPL9*, *RPL19*, *RPL26*, *RPL36*, *RPS14*, *RPS15*, and *RPS27A*, under conditions in which the Ct of s-q-PCR would occur within 1 cycle of that of the other primer sets (Tables 1 and 2). At the same time, we defined the criteria of a large deletion in our assay as follows. If multiple primer sets for one gene showed a 1-cycle delay from the other gene-specific primer set at the Ct score, we assumed that this represented a large deletion. As shown in Figure 1Bii and 1Cii, the specific primer sets for *RPL5* (L5-02, L5-05, L5-17, L5-19, and L5-28) detected a 1-cycle delay with respect to the mutated allele of patient 3. This assessment could be verified by simply confirming the difference of the cycles with the s-q-PCR amplification curves.

Study of large gene deletions in a Japanese DBA genomic DNA library

Sixty-eight Japanese DBA patients were registered and blood genomic DNA was collected at Hirosaki University. All samples were first screened for mutations in *RPL5*, *L11*, *L35A*, *S10*, *S14*, *S17*, *S19*, and *S26* by sequencing. Among these patients, 32.4% (22 of 68) had specific DBA mutations (Table 3 and data not shown). We then screened for large gene deletions in 27 patients from the remaining 46 patients who did not possess mutations as determined by sequencing (Table 4).

When we performed the s-q-PCR DBA gene copy number assay, 7 of 27 samples displayed a 1-cycle delay of Ct scores: 1 patient had *RPL5* (patient 14), 1 had *RPL35A* (patient 71), 3 had *RPS17* (patients 3, 60, 62), and 2 had *RPS19* (patients 24 and 72; Figure 2 and Table 4). Among these patients, the large deletions in the *RPL5* and *RPS17* genes are the first reported cases of allelic deletions in DBA. From these results, we estimate that a sizable number of Japanese DBA patients have a large deletion.

Based on our findings, the rate of large deletions was approximately 25.9% (7 of 27) in a category of unspecified gene mutations. Such mutations have typically gone undetected by conventional sequence analysis. We could not find any additional gene deletions in the analyzed samples.

Confirmation of the gene copy number for DBA genes by genome-wide SNP array

We performed genome-wide copy number analysis of the 27 DBA patients with a SNP array to confirm our s-q-PCR results. SNP array showed that patient 3 had a large deletion in

Table 4. Characteristics of DBA patients tested

Patient no.	Age at diagnosis	Sex	Hb, g/dL	Large deletion by s-q-PCR	Large deletion by SNP array	Inheritance	Malformations	Response to first steroid therapy
Patients with a large deletion in RP genes								
3*†	1 y	M		RPL5	RPL5	Sporadic	Short stature, thumb anomalies	Response
14*	5 y	M	5.5	RPS17	RPS17	Sporadic	White spots, short stature	Response
24*†	1 mo	F	5.5	RPS19	ND	Sporadic	Short stature, SGA	Response
60*†	2 mo	F	2.4	RPS17	RPS17	Sporadic	SGA	NT
62*†	1 mo	F	6.2	RPS17	RPS17	Sporadic	Small ASD, short stature, SGA	Response
71	0 y	M	5.3	RPL35A	RPL35A	Sporadic	Thumb anomalies, synostosis of radius and ulna, Cohelia Lange-like face, cleft palate, underdescended testis, short stature, cerebellar hypoplasia, fetal hydrops	NT
72†	0 y	M	2	RPS19	RPS19	Sporadic	Thumb anomalies, flat thenar, testicular hypoplasia, fetal hydrops, short stature, learning disability	No
Patients without a large deletion in RP genes								
5*	1 y	F	3.1	ND	ND	Sporadic	ND	Response
15*	1 mo	F	1.6	ND	ND	Sporadic	ND	Response
21*	1 y	F	2.6	ND	ND	Sporadic	ND	Response
26*	1 y 1 mo	F	8	ND	ND	Sporadic	Congenital hip dislocation, spastic quadriplegia, hypertelorism, nystagmus, short stature, learning disability	Response
33*	2 mo	F	1.3	ND	ND	Sporadic	ND	Response
36*	0 y	M	8.2	ND	ND	Familial	ND	Response
37*	4 y	M	6.1	ND	ND	Sporadic	Hypospadias, underdescended testis, SGA	NT
45*	5 d	M	5.1	ND	ND	Sporadic	Short stature, microcephaly, mental retardation, hypogammaglobulinemia	Poor
50*	2 m	F	3.4	ND	ND	Familial	ND	Response
61*	9 m	M	4	ND	ND	Sporadic	ND	Response
63*	0 y	M	6.8	ND	ND	Sporadic	Micrognathia, hypertelorism, short stature	Response
68	1 y 4 mo	M	5.9	ND	ND	Sporadic	ND	NT (CR)
69	1 y	M	9.3	ND	ND	Sporadic	ND	Response
76	0 y	M	4	ND	ND	Sporadic	ND	Response
77	0 y	M	7.8	ND	ND	Familial	Short stature	No
83	9 mo	F	3	ND	ND	Sporadic	ND	NT
90	10 mo	M	9	ND	ND	Sporadic	ND	No
91	0 y	F	3.8	ND	ND	Sporadic	ND	Response
92	2 mo	M	3.7	ND	ND	Sporadic	ASD, PFO, melanosis, underdescended testis, SGA, short stature	Response
93	11 mo	M	2.2	ND	ND	Sporadic	White spots, senile face, corneal opacity, underdescended testis, syndactyly, ectrodactyly, flexion contracture, extension contracture	Response

ND indicates not detected; NT, not tested; CR, complete remission; ASD, atrial septal defect; and PFO, persistent foramen ovale.

*Status data of Japanese probands 3 to 63 is from a report by Konno et al.[8]

†Large deletions of the parents of 5 DBA patients (3, 24, 60, 62, and 72) were analyzed by s-q-PCR, but there were no deletions in DBA genes in any of the 5 pairs of parents.

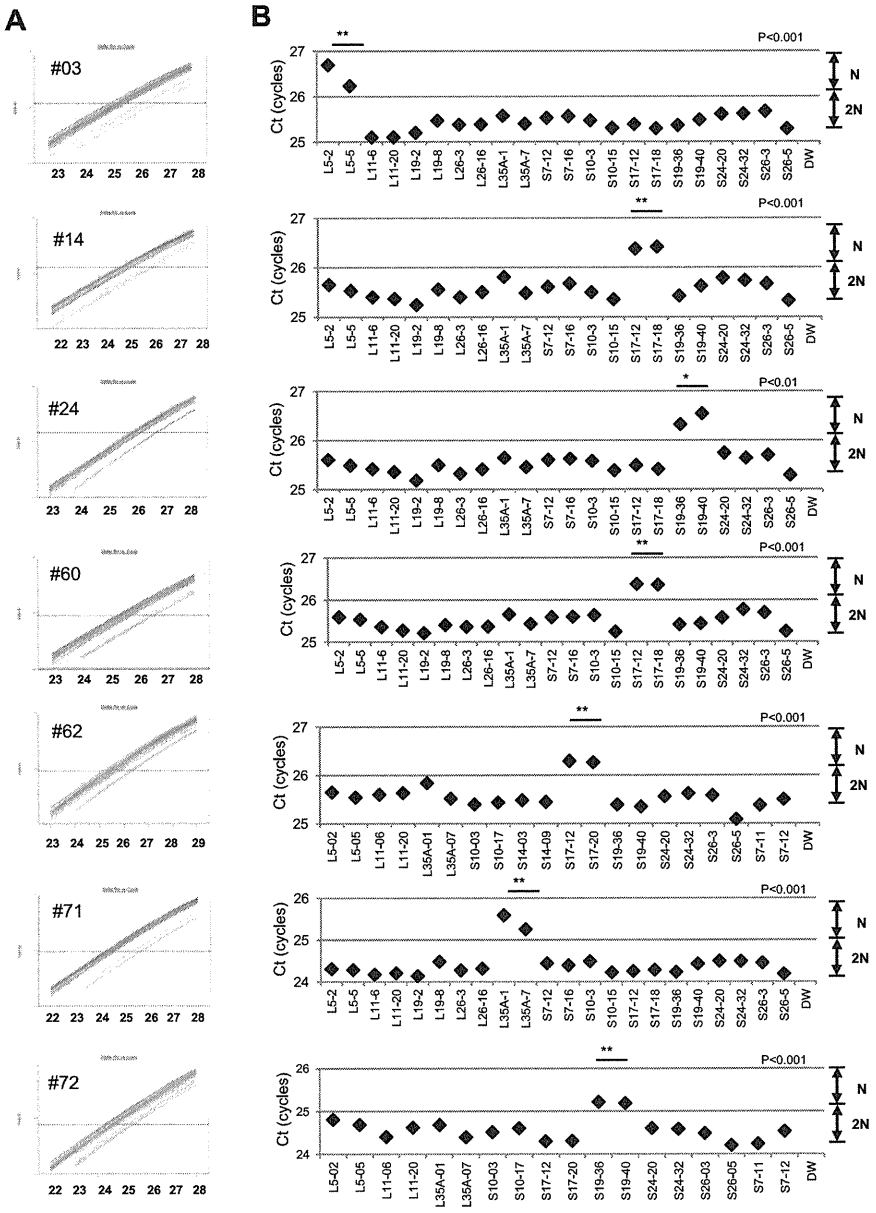

Figure 2. Detection of 7 mutations with a large deletion in DBA patients. Genomic DNA of 27 Japanese DBA patients with unknown mutations were subjected to the DBA gene copy number assay. (A) Amplification curve of s-q-PCR of a mutation with a large deletion. The deleted gene can be easily distinguished. (B) Ct score (cycles) of representative s-q-PCR with DBA genomic s-q-PCR primers. Results of the 2 gene-specific primer pairs indicated in the graph are representative of at least 2 sets for each gene-specific primer (carried out in the same run). $^{**}P < .001$; $^{*}P < .01$

chromosome 1 (ch1) spanning 858 kb (Figure 3A); patient 71 had a large deletion in ch3 spanning 786 kb (Figure 3B); patients 14, 60, and 62 had a large deletion in ch15 spanning 270 kb, 260 kb, and 330 kb, respectively (Figure 3C); and patient 72 had a large deletion in ch19 spanning 824 kb (Figure 3D). However, there were no deletions detected in ch19 in patient 24 (Figure 3D). Genes estimated to reside within a large deletion are listed in supplemental Table 1. Consistent with these s-q-PCR results, 6 of 7 large deletions were detected and confirmed as deleted regions, and these large deletions contained *RPL5*, *RPL35A*, *RPS17*, and *RPS19* (Table 4 and supplemental Table 1). Other large deletions in RP genes were not detected by this analysis. From these results, we conclude that the synchronized multiple PCR amplification method has a detection sensitivity comparable to that of SNP arrays.

Detailed examination of a patient with intragenic deletion in the RPS19 allele (patient 24)

Interestingly, for patient 24, in whom we could not detect a large deletion by SNP array at s-q-PCR gene copy number analysis, 2 primer sets for *RPS19* showed a 1-cycle delay (RPS19-36 and RPS19-40), but 2 other primer pairs (RPS19-58 and RPS19-62) did not show this delay (Figure 4A). We attempted to determine the deleted region in detail by testing more primer sets on *RPS19*. We tested a total of 9 primer sets for *RPS19* (Figure 4B) and examined the gene copy numbers. Surprisingly, 4 primer sets (S19-24, S19-36, S19-40, and S19-44) for intron 3 of *RPS19* indicated a 1-cycle delay, but the other primers for *RPS19* located on the 5′untranslated region (5′UTR), intron 3, or 3′UTR did not show this delay (S19-57, S19-58, S19-28, S19-62, and S19-65; Figure 4B-C). These results suggest that the intragenic deletion occurred in the *RPS19* allele. To confirm this deleted region precisely, we performed genomic PCR on *RPS19*, amplifying a region from the 5′UTR to intron 3 (Figure

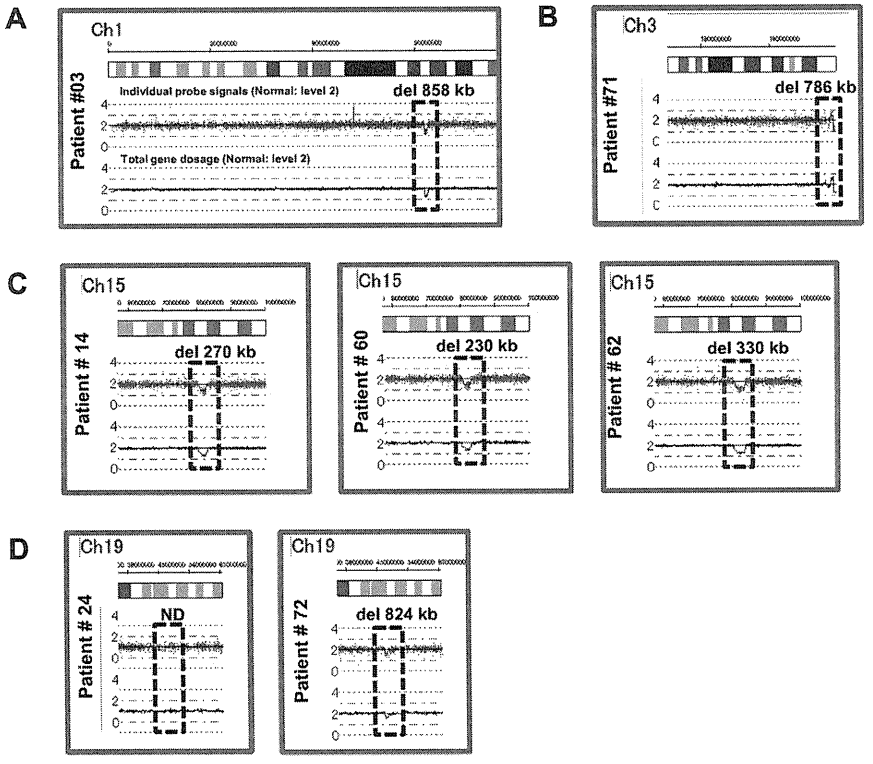

Figure 3. Results of SNP genomic microarray (SNP-chip) analysis. Genomic DNA of 27 Japanese DBA patients with unknown mutations was examined using a SNP array. Six patients had large deletions in their chromosome (ch), which included one DBA-responsible gene. Patient 3 has a large deletion in ch1 (A), patient 71 has a deletion in ch3 (B), patients 14, 60, and 62 have deletions in ch15 (C), and patient 72 has a deletion in ch19 (D).

4B). In patient 24, we observed an abnormally sized PCR product at a low molecular weight by agarose gel electrophoresis (Figure 4D). We did not detect a wild-type PCR product from the genomic PCR. This finding is probably because PCR tends to amplify smaller molecules more easily. However, we did detect a PCR fragment at the correct size using primers located in the supposedly deleted region. These bands were thought to be from the products of a wild-type allele. Sequencing of the mutant band revealed that intragenic recombination occurred at a homologous region of 27 nucleotides, from −1400 to −1374 in the 5′ region, to +5758 and +5784 in intron 3, which resulted in the loss of 7157 base pairs in the *RPS19* gene (Figure 4E). The deleted region contains exons 1, 2, and 3, and therefore the correct *RPS19* mRNA could not be transcribed.

Genotype-phenotype analysis and DBA mutations in Japan

Patients with a large deletion in DBA genes had common phenotypes (Table 4). Malformation with growth retardation (GR), including short stature or SGA, were observed in all 7 patients. In patients who had a mutation found by sequencing, half had GR (11 of 22; status data of DBA patients with mutations found by sequencing are not shown). GR may be a distinct phenotypic feature of large deletion mutations in Japanese DBA patients. Familial mutations were analyzed for parents for 5 DBA patients with a large deletion (patients 3, 24, 60, 62, and 72) by s-q-PCR. There are no large deletions in all 5 pairs of parents in DBA-responsible genes. Four of the 7 patients responded to steroid therapy. We have not observed significant phenotypic differences between patients with extensive deletions and other patients with regard to blood counts, responsiveness to treatment, or other malformations.

Discussion

Many studies have reported RP genes to be responsible for DBA. However, mutations have not been determined for approximately half of DBA patients analyzed. There are 2 possible reasons for this finding. One possibility is that patients have other genes responsible for DBA, and the other is that patients have a complicated set of mutations in RP genes that are difficult to detect. In the present study, we focused on the latter possibility because we have found fewer Japanese DBA patients with RP gene mutations (32.4%) compared with another cohort study of 117 DBA patients and 9 RP genes (approximately 52.9%).[4] With our newly developed method, we identified 7 new mutations with a large deletion in *RPL5*, *RPL35A*, *RPS17*, and *RPS19*.

The frequency of a large deletion was approximately 25.9% (7 of 27) in our group of patients who were not found to have mutations by genomic sequencing. Therefore, total RP gene mutations were confirmed in 42.6% of these Japanese patients (Table 5). Interestingly, mutations in *RPS17* have been observed at a high rate (5.9%) in Japan relative to that in other countries (1%).[5,15,16] Although the percentage of DBA mutations differs among different ethnic groups,[8,17-19] a certain portion of large deletions in DBA-responsible genes are likely to be determined in other countries by new strategies.

In the present study, we analyzed patient data to determine genotype-phenotype relations. To date, large deletions have been reported with RPS19 and RPL35A in DBA patients.[3,6,13] *RPS19* large deletions/translocations have been reported in 12 patients, and *RPL35A* large deletions have been reported in 2 patients.[19] GR in patients with a large deletion has been observed previously with *RPS19* translocations,[3,19-21] but it was not found in 2 patients with *RPL35A* deletion.[6] Interestingly, all of our patients with a large deletion had a phenotype

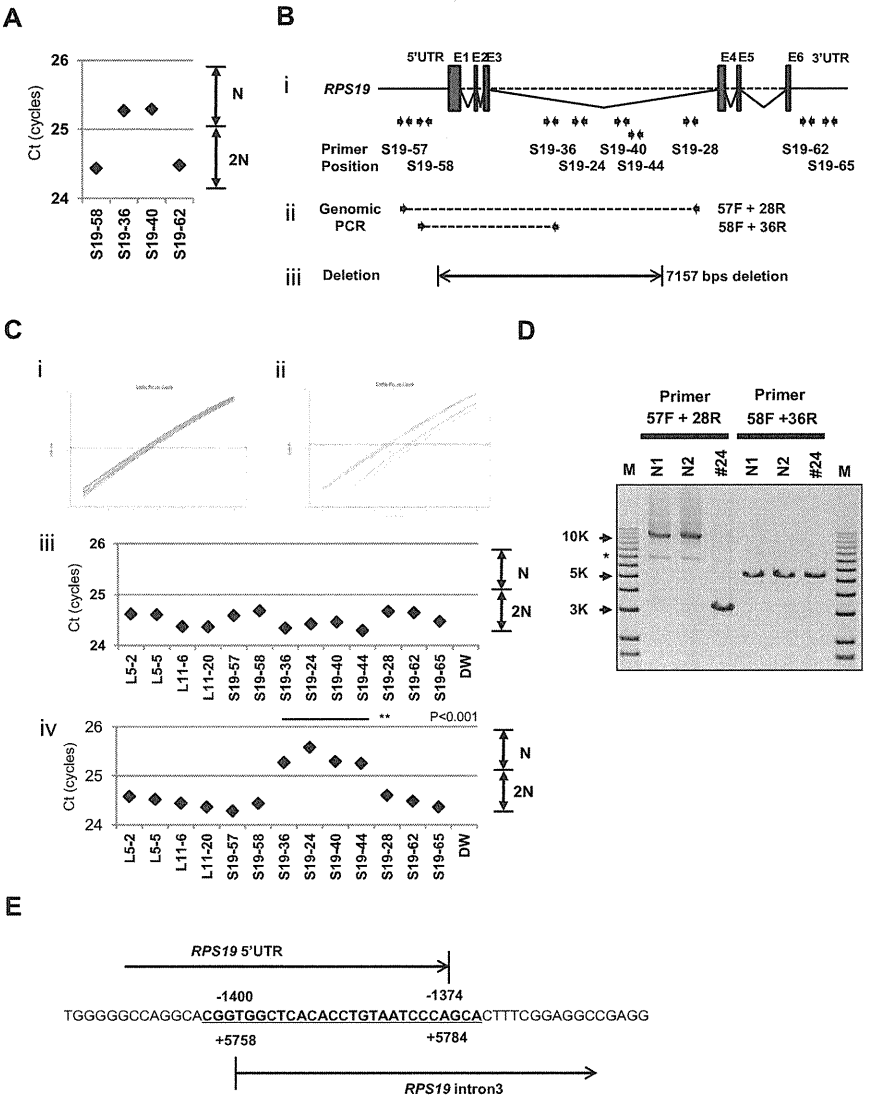

Figure 4. Result of s-q-PCR gene copy number assay for patient 24. (A) Results of s-q-PCR gene copy number assay for *RPS19* with 4 primer sets. (Bi) The *RPS19* gene copy number was analyzed with 9 specific primer sets for *RPS19* that span from the 5′UTR to the 3′UTR. (ii) Primer positions of genomic PCR for *RPS19*. (iii) Region determined to be an intragenic deletion in *RPS19*. (C) Results of gene copy number assay for *RPS19* show a healthy person (i,iii) and a DBA patient (ii,iv), and Ct results are shown (iii-iv). Patient 24 showed a "1-cycle delay" with primers located in the intron 3 region, but other primer sets were normal. (D) Results of genomic PCR amplification visualized by agarose gel electrophoresis to determine the region of deletion. N1 and N2 are healthy samples. *Nonspecific band. (E) Results from the genomic sequence of the 3-kb DNA band from genomic PCR on patient 24 showing an intragenic recombination from −1400 to 5784 (7157 nt) in *RPS19*. $^{**}P < .001$.

of GR, including short stature and SGA, which suggests that this is a characteristic of DBA with a large gene deletion in Japan. Our study results suggest the possibility that GR is associated with extensive deletion in Japanese patients. Although further case studies will be needed to confirm this possibility, screening of DBA samples using our newly developed method will help to advance our understanding of the broader implications of the mutations and the correlation with the DBA genotype-phenotype.

Table 5. Total mutations in Japanese DBA patients, including large gene deletions

Gene	Mutation rate
RPS19	12(17.6%)
RPL5	7(10.3%)
RPL11	3 (4.4%)
RPS17	4 (5.9%)
RPS10	1 (1.5%)
RPS26	1 (1.5%)
RPL35A	1 (1.5%)
RPS24	0
RPS14	0
Mutations, n (%)	29(42.6%)
Total analyzed, N	68

Copy number variation analysis of DBA has been performed by linkage analysis, and the *RPS19* gene was first identified as a DBA-susceptibility gene. Comparative genomic hybridization array technology has also been used to detect DBA mutations in *RPL35A*, and multiplex ligation-dependent probe amplification has been used for *RPS19* gene deletion analysis.[3,6,13,22] However, these analyzing systems have problems in mutation screening. Linkage analysis is not a convenient tool to screen for multiple genetic mutations, such as those in DBA, because it requires a high level of proficiency. Although comparative genomic hybridization technology is a powerful tool with which to analyze copy number comprehensively, this method requires highly specialized equipment and analyzing software, which limits accessibility for researchers. Whereas quantitative PCR–based methods for copy number variation analysis are commercially available (TaqMan), they require a standard curve for each primer set, which limits the number of genes that can be loaded on a PCR plate. To address this issue, a new method of analysis is needed. By stringent selection of PCR primers, the s-q-PCR method enables analysis of many DBA genes in 1 PCR plate and the ability to immediately distinguish a large deletion using the s-q-PCR amplification curve. In our study, 6 of 7 large deletions in the RP gene detected by s-q-PCR were confirmed by SNP arrays (Figure 3). Interestingly, we detected